

**\*\*\* Chapter 2 \*\*\***

## 2.1 Experimental Set-up :

*Extensive air shower (EAS)* is an unique means for the study of cosmic rays of energies greater than  $10^{14}$  eV. From the fifties the study of extensive air showers using large arrays of particle detector has been made for the interest of high energy physics in the region not accessible in accelerators and also for the study of the characteristics of primary ultra high energy (UHE) cosmic rays. Since the convincing discovery of UHE gamma radiation from Cygnus X-3 by the Kiel group air shower arrays are extensively used in the search for point sources of cosmic rays.

The air shower initiated by a cosmic ray particle or a gamma ray photon in the energy range  $10^{14}$  to  $10^{16}$  consist of about  $10^4$  to  $10^6$  particles at sea level. The particles present in an EAS may be classified into three groups, electromagnetic component or soft component which consists of electrons, positrons and photons, muon component and hadronic component. The particles of the electromagnetic and muon components are spread over a large area with density of particles decreases rapidly as the radial distance from the shower core increases. The shower front can be sampled with a large number of particle detectors regularly spread over a wide distance range.

### The NBU EAS array :

The small air shower array at North Bengal University campus (latitude  $26^{\circ}42'$  N, longitude  $88^{\circ}21'$  E, 150 m a.s.l., atmospheric depth  $1015 \text{ gm}^{-2}$ ), INDIA, operating since 1982. At present it is composed of nineteen plastic scintillation counter, each of area  $0.25 \text{ m}^2$ , for the measurement of density of electronic component of air shower, eight fast timing counters to determine the arrival direction of primary cosmic ray particles and two magnet spectrographs of maximum detectable momentum  $220 \text{ GeV}/c$ . The scintillation counters are arranged in a radial symmetric pattern around the centre of the array with a spacing of about 8 m near the array centre and a spacing of about 16 m at the edge of the array. The plan of the array is shown in fig 2.1.1. The total area covered by the array is about  $1600 \text{ m}^2$ . The array is designed to observe showers of energies  $10^{14} - 10^{17}$  eV. Timing informations are obtained from eight fast timing detectors, four of them located near the centre of the array while the rest four are placed at the edge of the array. Two magnetic spectrographs, each of an area  $0.5 \text{ m}^2$ , under a concrete shielding absorber are also

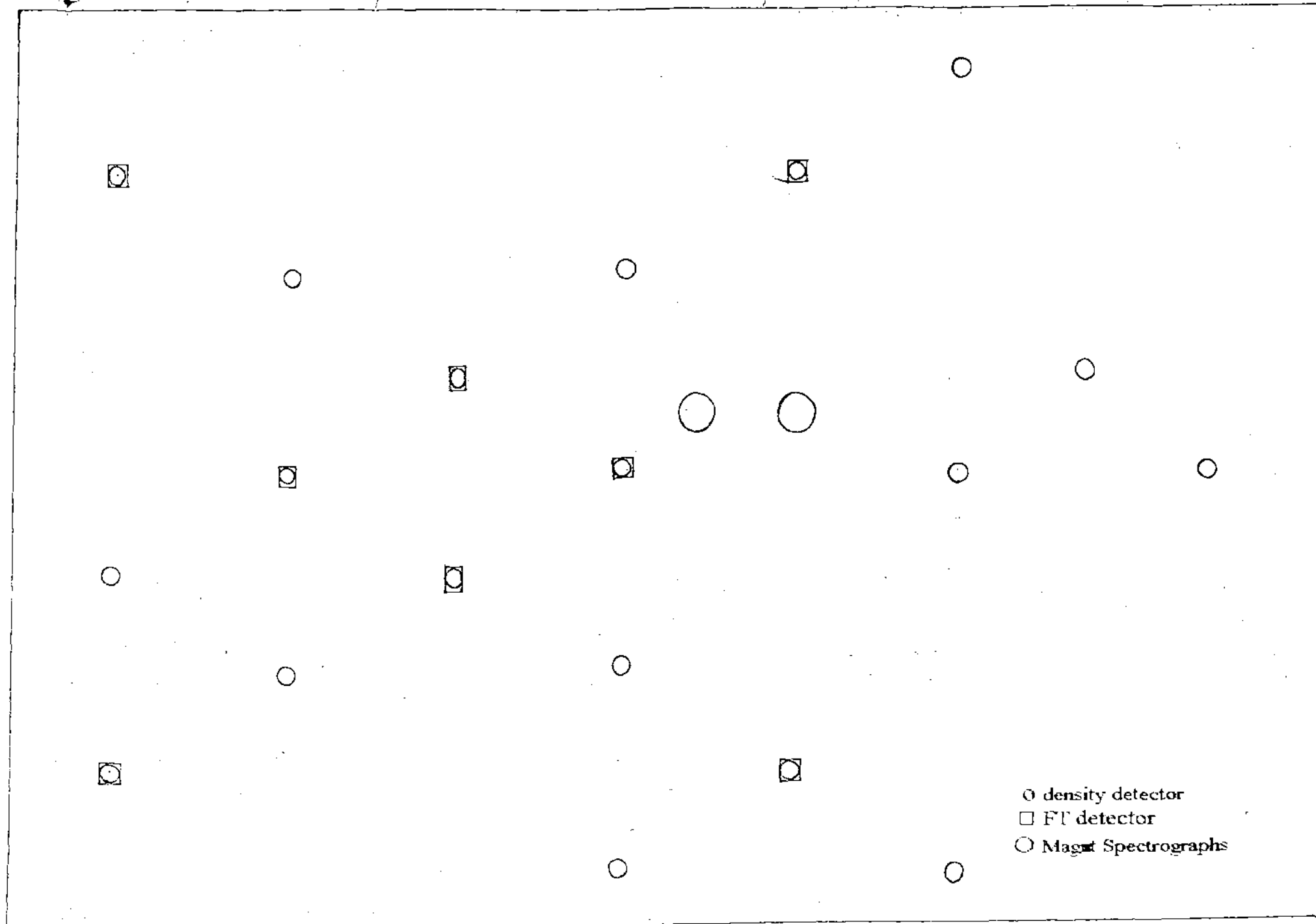


Fig 2.1.1 The NBU EAS array

← 4 m →

operated in conjunction with the air shower array for the study of muon component of EAS.

### Electron density detectors :

In the NBU air shower experiment plastic scintillation counters are used as particle detector for obtaining the density information of the soft component of the EAS. In each detector a 50 cm x 50 cm plastic scintillator with thickness 5 cm is housed in a pyramidal light tight enclosure made by galvanized iron sheet and viewed from below by a photomultiplier ( Philips XP 2050 / Dumont 6364 / RCA 5819 ) from a vertical distance of about 39 cm (Fig.2.1.2). The inner surfaces of the enclosure are painted with high reflection efficiency material composed of Titanium dioxide ( $TiO_2$ ). The photomultiplier tubes are operated in the voltage range 850 - 1200 volt. Different voltages have to be applied to different counters to ensure that the single particle pulse height in different counters are nearly same. The detectors were calibrated for cosmic ray muons. This was done by placing each scintillation counter within a telescopic arrangement of three GM counters, two of which were placed above the detector with their axis mutually perpendicular to each other and the third GM counter was placed below the detector. The variation in the detecting efficiency of the scintillation detectors from the centre of the detector to its edge found small ( $< 8\%$ ), probably due to small size of the detectors.

### Fast timing detectors

Fast timing system is one of the important part of the NBU air shower array in order to determine the arrival direction of primary cosmic ray and to investigate the characteristics of EAS at various inclinations. Eight timing detectors are employed in the NBU array to get the timing information of shower front. The shape and size of the scintillator and the enclosure of these timing detectors are the same as electron density detectors. But Philips fast photomultiplier tubes (XP 2020, rise time  $\sim 1.5$  ns) are used instead of relatively slow photomultipliers (rise time  $\sim 20 - 30$  ns) used in the electron density detectors. These photomultiplier tubes are operated at negative voltages of 2000 - 2200 volts to minimise the noise generated from the high voltage power supply.

### The magnet spectrographs :

Two magnetic spectrometers are operated in conjunction with the NBU EAS array to study

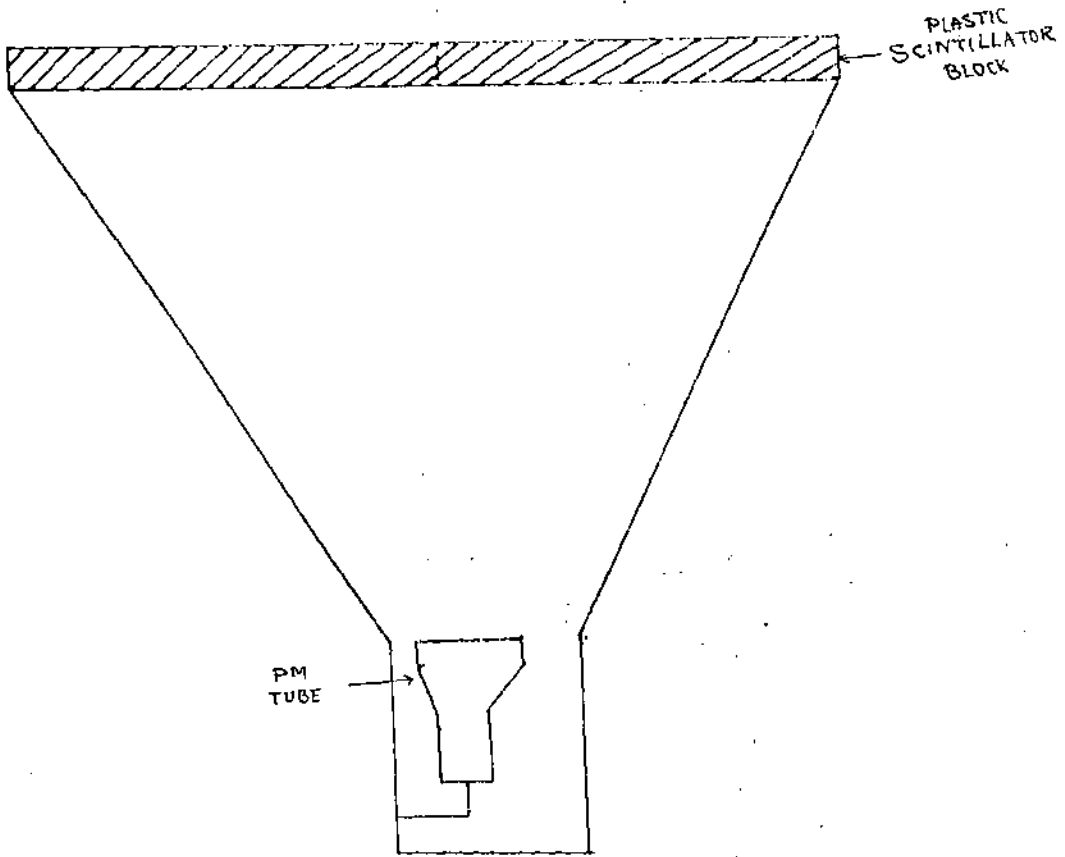


Fig. 2.1.2. SCINTILLATION DETECTOR ASSEMBLY.

---

the muon component of the EAS. The spectrograph consists of a solid iron magnet in between four neon flash tube trays. The solid iron is built by placing 80 low carbon content steel plates (180 cm x 125 cm x 1.25 cm) having a rectangular hole (35 cm x 19 cm) at the centre, one above another. The height of the iron yoke of the spectrometers (the maximum path of a muon in magnetic field) is 1 m. the magnetic induction in iron is  $B = 16$  Kgs. To filter out the electromagnetic component the spectrograph is shielded by concrete absorber. Additional lead absorber of about 5 cm thickness is placed above the top tray of the neon flash tubes to increase the absorbing capability of the electronic component. The solid iron magnet itself acts as a absorber. As a result the lower energy cut-off for the incident particle is set at 2.5 GeV. The neon flash tubes are placed in a hodoscopic arrangement which are used as muon track detectors. Two flash tube trays are placed above each magnet while two are placed below in such a way that if a muon is detected by the system then the muon have to pass through all the four neon tube hodoscope. The accuracy of locating a muon trajectory is within  $\pm 0.14$  cm. Four cameras are used for recording the muon trajectories from the flashes of the muon tubes. The muon energy is determined on the basis of muon deflection in magnetic field. The magnetic spectrographs limit the zenith angle of acceptance of the incident muons to a few degrees from the vertical. The detailed of the spectrograph is available in (1).

#### Data Acquisition System :

Data acquisition system is an essential part of any EAS array. In the NBU setup data acquisition system plays a very important role. It first selects an air shower event and when an air shower event occurs it records the event time, the density information in each particle detector and timing information in each fast timing counter. It also records the muon trajectories in magnetic spectrographs if spectrographs detect muons in coincidence with the air shower trigger. The whole data handling system may be divided into four main parts, a EAS selection system (coincidence circuit), timing data handling system, density data handling system and muon data handling system.

#### 1. EAS selection system :

In the present experiment an air shower event is selected only when a minimum of four particles per square meter incident within 50 ns in each of the four triggering detectors located near the centre of the array. An EAS selection or trigger circuit is used to generate a fast trigger pulse

whenever the arriving shower satisfy the shower selection criteria.

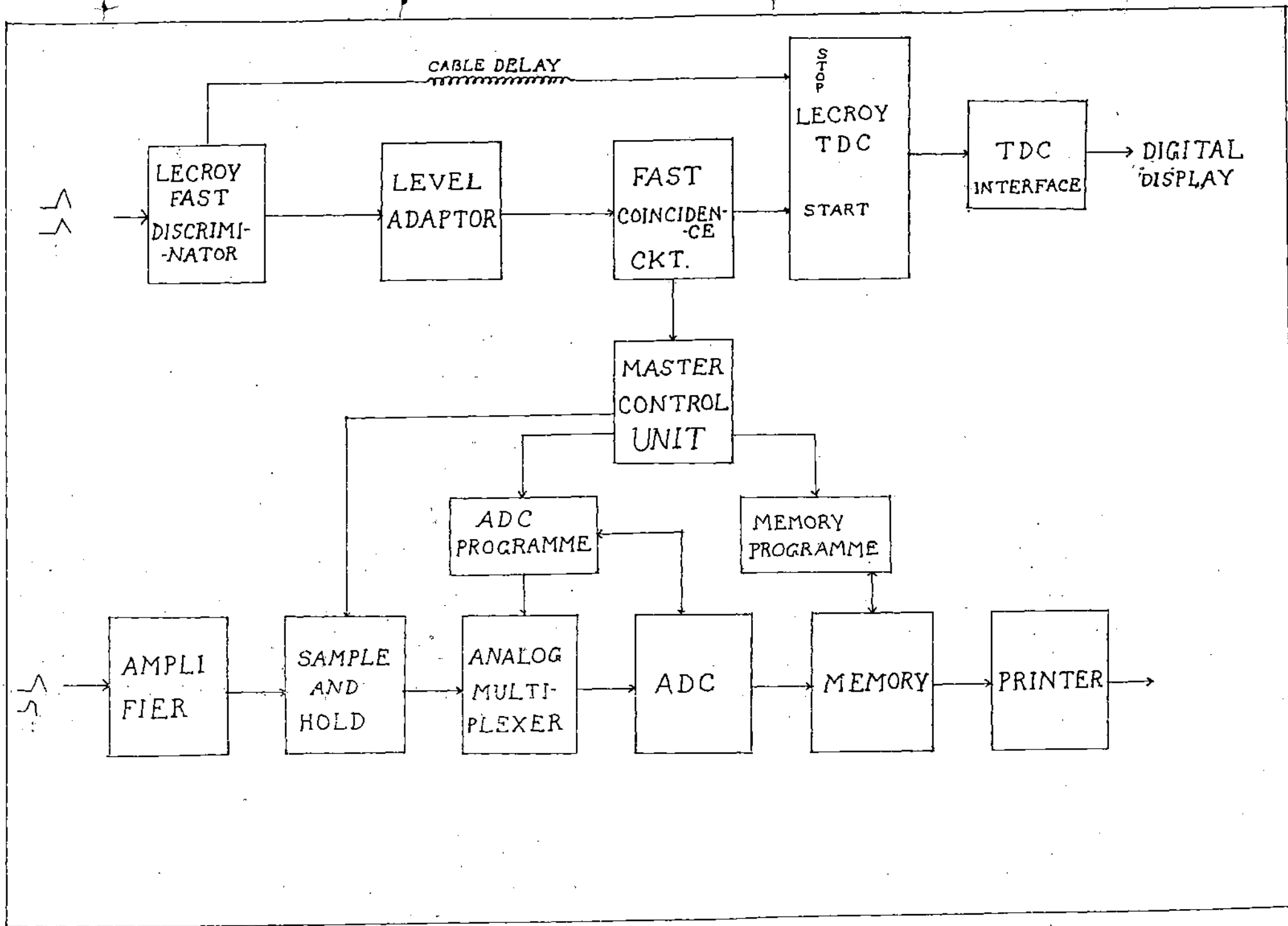
## 2. Timing data handling system :

The output pulses from the all first timing detectors are brought to the control room which is located near the centre of the array by means of nearly equal length coaxial cables (RG 58) . Then these pulses are given to a *Lecroy fast discriminator* (Lecroy octal discriminator 62J B). The width of the discriminator output pulse is adjusted to 50 ns which ensure that a coincidence always takes place between timing pulses from four central detectors when a shower having size greater than the threshold size, incident within the effective area of the array. The bias of the discriminator is set at half particle level. The fast discriminator outputs are given to a fast coincidence circuit and this coincidence output pulse is used as the start pulse for the eight channel *Lecroy TDC* modules (Lecroy 2228 A) . Outputs of the each discriminator channel is delayed by 172 feet RG 174 cables (total delay nearly 258 ns) and these delayed pulses give the individual TDC stop. From the TDC data the relative arrival times of the shower particles at various points are obtained.

## 3. Density data handling system :

From each particle density counters essentially the pulse height information is obtained. Knowing average single particle pulse height the number of charged particles traversing the counter can be calculated. To digitise the analogue pulses carrying the information of charged particle density in EAS at various points a *Wilkinson type Analogue to Digital Convertor* (ADC) (2) is used.

The output pulses from each particle detector are brought to the main control room through RG-58 co-axial cables using preamplifiers which sit below the photomultipliers of the scintillation counters. These preamplifier outputs are amplified in the control room and fed to the *Sample and Hold* (S/H) (3) circuits. The *sample and hold* circuit holds the peak of the pulse normally for about 3  $\mu$ s by charging a capacitor. At the end of 3  $\mu$ s duration the capacitor is discharged and the S/H circuit is ready to accept the next event. Whenever an air shower hits the array and the trigger condition of the array is met a master trigger pulse is generated. This master pulse triggers the *Master Control Unit* (MCU) of the data handling system which in turn generates a set of instructions. It gives a hold command to all the S/H circuits, switches off the input data lines by



Block Diagram of the Data Handling System.

analogue switches and triggers the ADC programme circuit simultaneously. The master pulse is also used for the veto of the coincidence circuit. The veto is withdrawn only after the recording of the event time, the timing informations and the density informations. According to the instruction the S/H circuits hold the input informations at that instant till the the hold command is withdrawn. Now the ADC programme unit connects all the output pulses of the S/H circuits by an analogue multiplexer to the ADC system one after another. It first selects the first channel of the analogue multiplexer and connects it to the ADC system for digitization of the analogue pulse. Once the conversion is over the digitised output of ADC is read into the memory unit. Next the second channel of the *analogue multiplexer* is selected and the same process repeat. The total time required to scan all the density channels is about 8 ms. After the storage of all the density information for all the density detectors in memory unit these data are transferred to the printer for printing on a paper tape.

#### 4. Muon data handling system :

For the detection of muons a telescopic arrangement of scintillation counters are used. Each spectrographs unit is placed in between the two scintillation counters. When a muon passes through the telescope a two fold coincidence pulse is generated. If this twofold coincidence pulse occurs in coincidence with the air shower trigger a high voltage pulse of about 4.5 KV/cm of rise time .75  $\mu$ s ( $\mu$ s) is applied to the aluminum electrodes placed between the layers of the Neon flash tubes within the 5  $\mu$ s of the passage of the muon. In the influence of the high energy muon that passes through the spectrographs the Neon flash tubes on its trajectory are ionised and glow with the application of high voltage pulse. Four cameras are used for recording the muon trajectory from the flashes of the Neon tubes.

All the detectors of the array and the data handling system are monitored daily and sequentially.

Modernisation and extension of the existing NBU array has been completed. In the present form the old data handling system is replaced by a fast computer interfaced data handling system. The accuracy in measurement of event time has been improved a lot. Computer hard disks and floppy disks are now used instead of paper tape as storage device of the EAS events.

## 2.2 Data treatment and analysis:

Recorded EAS events are analysed to obtain astrophysical and nuclear physical informations associated with the EAS data. There are a number of observable shower parameters which provide various information about the primary cosmic rays and about the shower development. Estimation of shower parameters is a necessary preliminary in shower analysis. In the current analysis the following routine for estimation of shower parameters has been used.

1. Initial estimation of arrival direction of showers.
2. Estimation of four basic shower parameters viz. core location  $(x_0, y_0)$ , shower size  $(N_e)$  and shower age parameter(s).
3. Re-estimation of the arrival angle of shower considering the shower front curvature and the thickness of the shower disk.

Muon data are analysed separately.

Showers are selected for the current analysis if they have

- (i) core location within thirty meter from the array center (approximately the array boundary)
- (ii) at least five detectors with particle density greater than four per square meter
- and (iii) at least four timing measurements of the shower front.

### 1. Estimation of arrival angles of incident EAS :

An exact determination of arrival direction of showers is important to identify the ultra high energy point sources. The accuracy of the arrival angle determination mainly depends on the capability of accurate measurement of the relative arrival times of the shower particles. The uncertainty in the timing measurement causes by several factors, time spreads of the shower particles in the shower disk, curvature of the shower front, Instrumental uncertainty of the time measuring instruments, time offsets etc.

### Instrumental uncertainty in timing measurement :

Due to the finite precision of the time measuring instruments used in making the arrival time measurements of the shower particles an uncertainty is introduced in the final directional results. This inherent uncertainty is known as Instrumental uncertainty and is an important

parameter in the directional study. In the present experiment the Instrumental uncertainty is measured in the following way.

The fast timing detector under study is placed above another fast timing scintillation detector thus forming a telescope. Coincidence is taken between the two detectors and this coincidence pulse is used to start the TDC. The pulses from the individual detectors are fed into Discriminator and the output pulses of the Discriminator are given same amount of cable delay. These delayed pulses are used to stop the individual channels of the TDC. If  $t_d$  is the time recorded by the detector under study when a particle passes through the telescope,  $t_0$  is the time measured by the other fast detector of the telescope for the same event and  $d$  is the vertical distance between them then in ideal cases the quantity  $\delta = t_d - t_0 + d/c$  should be zero but in practice only the average of  $\delta$  for a large number of observations is <sup>found</sup> ~~appeared~~ to be nearly zero. A distribution is formed for the quantity  $\delta$  which is shown in fig 2.2.1. The standard deviation  $\sigma$  for the Gaussian fitting of this distribution gives the uncertainty in the arrival time measurement. Since the uncertainty for two detectors combine ( quadratically ) in the estimation of  $\sigma$  the uncertainty in the timing measurement for a single detector is  $\sigma / 2^{.5}$  which is in the present case  $1.22 \pm .03$  ns.

#### Time offsets of the time measuring instruments :

There may be a finite but constant difference in the actual time of arrival of a shower particle in a fast timing detector and the measured time by the detector. This difference in time is known as time offset of the timing detector. The amounts of offsets are different for different time measuring instruments. Since the actual arrival times of shower particles are necessary to obtain true arrival direction of showers, the measured times have to be corrected for the time offsets before they are used for the directional analysis. The arrival direction of an air shower event is normally determined by the fast timing technique. Using this technique the arrival directions are practically determined by the relative arrival times of the shower particles on each fast timing detector. So only the relative time offsets between the different timing instruments are necessary, not the actual time offsets of the instruments. During the experiment different voltages have to be applied to photomultipliers of the different fast timing detectors. This causes different photomultiplier transit time in different detectors. There may be a small difference in the response time of the scintillators and/or photomultipliers of the different detectors. A small difference in cable delay between different channels may exist due to unequal cable length (which is obviously very small)

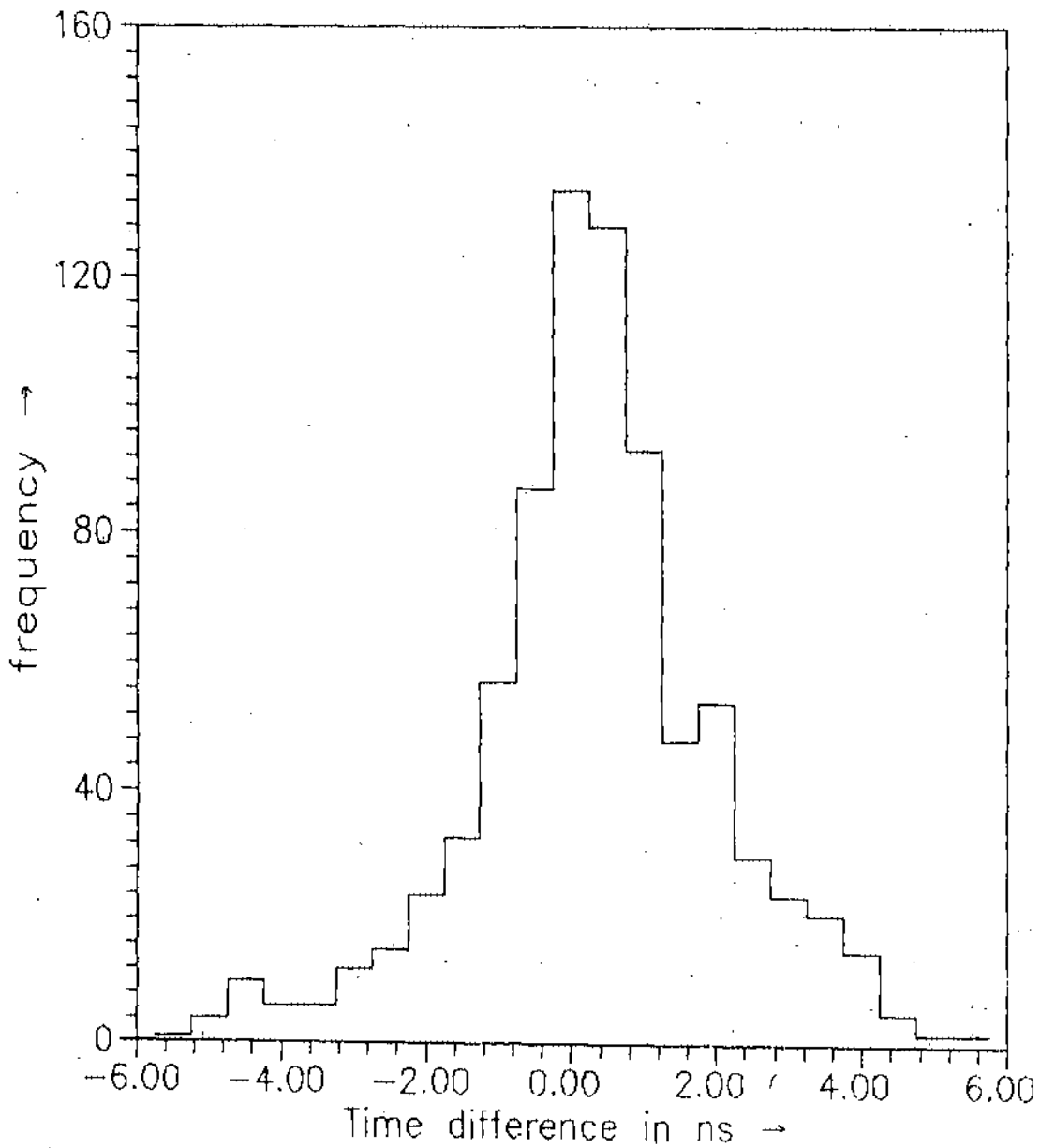


Fig. 2.2.1 Distribution of the deviations in arrival times between two fast timing detectors.  
(Average =  $.34 \pm .06$  , St. Deviation =  $1.73 \pm .04$ )

or any manufacturing differences of cables. There might be a small difference in electronic propagation delay between different time measuring channel. These factors are responsible for the relative time offsets of the time measuring instruments. In the present experiment the relative time offsets are determined in the following way.

Suppose  $t_i$  is the true arrival time of a shower particle in the  $i$ th detector. Time response delay of the detector, electronic propagation delay, cable delay etc causes a total  $to_i$  amount of delay, so that time measured by the detector will be  $t_i^m = t_i + to_i$ . Here  $to_i$  is the true time offset of the  $i$ th time measuring instrument. Similarly time measured by the  $j$ th detector will be  $t_j^m = t_j + to_j$ .

Therefore

$$t_i^m - t_j^m = t_i - t_j + to_i - to_j$$

$to_i - to_j$  is the relative time offsets between the  $i$ th and  $j$ th timing instruments. The summation of the quantity  $t_i^m - t_j^m$  is taken for a large number of events. For a large number of events the quantity  $\Sigma (t_i - t_j)$  should vanish provided the observed events have azimuthal isotropy (which is expected because of the highly isotropic nature of the cosmic rays). Hence for each pair of detectors we get

$$\Sigma (to_i - to_j) = \Sigma (t_i^m - t_j^m)$$

or

$$(to_i - to_j - t_{ij}^m) = 0$$

where

$$t_{ij}^m = 1/n \Sigma (t_i^m - t_j^m)$$

$n$  is the total number of events considered. There are eight such equations for eight detectors. Solution of these equations gives the relative time offsets between different detectors.

#### Initial estimation of EAS direction :

Initial estimation of shower direction is found by a unweighted least square fit of a plane shower front to the timing data. If a detector is not fired in a shower event it will make no

contribution to the calculation of the shower directions. The plane shower front is given by

$$l x_i + m y_i + n z_i + c (t_i - t_0) = 0 \quad \dots \quad 1$$

where  $x_i, y_i, z_i$  are the coordinates of the  $i$ th detector,  $t_i$  is the arrival time of a shower particle on the  $i$ th detector,  $l, m, n$  are the direction cosines and  $t_0$  is a reference time which is actually the time of arrival at a fictitious detector at the origin of the coordinate system. The direction cosines are constrained by the relation

$$l^2 + m^2 + n^2 = 1 \quad \dots \quad 2$$

The quantity

$$\chi^2 = \sum w_i \{ l x_i + m y_i + n z_i + c (t_i - t_0) \}^2 \quad \dots \quad 3$$

where the summation is over all the detectors producing time information of the shower front for that particular event, is minimised to determine the free parameters  $l, m, n$  and  $t_0$ . The  $w_i$ 's are the weight factors all of which are taken 1 in the initial estimation of shower direction. The conditions of minimization of  $\chi^2$  with respect to  $l, m, n$  and  $t_0$  are given by

$$\delta \chi^2 / \delta l = 0$$

$$\delta \chi^2 / \delta m = 0$$

$$\delta \chi^2 / \delta n = 0$$

and 
$$\delta \chi^2 / \delta t_0 = 0$$

Solution of these equations along with the constrained condition of direction cosines (eqn. no. 2) gives the values of  $l, m, n$  and  $t_0$  in terms of spatial coordinates of the timing detectors and the arrival times of the shower particles at different detectors. The measured arrival times of the

shower particles are corrected for the offset of the corresponding detector before analysis of arrival direction. Thus the direction cosines and hence zenith angle ( $z$ ) and azimuthal angle ( $A$ ) of each shower event is determined.

## 2. Determination of shower parameters :

Estimation of basic shower parameters is a necessary preliminary in shower analysis. The shower core ( $x_0, y_0$ ), shower size ( $N_e$ ) and shower age parameter ( $s$ ) are normally treated as basic shower parameters. The shower core is a point in the shower plane having maximum shower particle density. The shower size gives the total number of shower particles present in the shower at the observation level and the shower age parameter describe the longitudinal development of electromagnetic cascade. Since most of the shower particles are electron and photons, basic shower parameters are determined by the electromagnetic components. There is no direct way of determination of these shower parameters. These parameters are usually estimated in an indirect way by fitting the experimentally observed shower particle densities to a lateral distribution function (ldf) of shower particles. Thus ldf of the soft component of the EAS plays a very important role in the study of cosmic ray air showers. The shape of the distribution is also important by itself since it gives information about the model of shower development. So knowledge of the ldf of the soft component of the EAS is a prerequisite for the analysis of showers detected with scintillation counters.

Different authors proposed different functional forms of the lateral distribution of the electromagnetic component of EAS but till now there is no one functional form of general acceptance. Basic analytical work in this field is due to Moliere(1). However Moliere distribution is only applicable near the maximum development of the cascade. Nishimura and Kamata (2) extended the earlier work and obtained a distribution for all stages of development. Greisen (3) put forward an empirical relation representing the Nishimura and Kamata distribution which is the well-known NKG function and is given by

$$\rho(r) = c(s) N_e (r/r_m)^{s-2} (1 + r/r_m)^{s-4.5}$$

where  $\rho(r)$  is the density of shower particles at radial distance  $r$  from the shower core,  $s$  is the shower age parameter,  $N_e$  represents the shower size,  $r_m$  is the Moliere radius and  $c(s)$  is the normalisation constant which is given by

$$c(s) = 1/(2\pi r_m^2) \Gamma(4.5 - s) / \{\Gamma(s) \Gamma(4.5 - 2s)\}$$

The NKG function has been widely used in the analysis of electron density data of air showers. However for several years, a number of authors has pointed out that the NKG function does not give a good description of the electron lateral distribution of air showers. Now there is consensus among the researchers of the field that the correct lateral distribution is substantially narrower than the NKG function. But the NKG function as a whole seems better than the other lateral distribution functions in interpreting the experimental data. Moreover most of the cosmic ray groups are using NKG function to analyse their air shower data in connection with the search for UHE radiation from discrete point sources. To compare the results of the present experiment with the results of other EAS experiments it is necessary to use the same lateral distribution function of electrons for estimation of the shower parameters. So considering the above factors, in the present analysis we use NKG function as lateral structure function for electronic component of air showers.

The main parameters of individual EAS were determined using a computer. The density informations of shower particles at different detectors are obtained from the ADC readings. The shower parameters i.e, the core location  $(x_0, y_0)$ , shower age  $(s)$  and shower size  $(N_e)$  have been determined by minimising a weighted chi-square ( $\chi^2$ ) which is defined as follows

$$\chi^2 = \sum W_i (\Delta_i^o - \Delta_i^e)$$

where  $\Delta_i^o$  is the observed density in the  $i$ th particle detector which is related to the corresponding ADC reading  $D_i$  by the relation

$$\Delta_i^o = D_i / (A_i \times C_i)$$

$A_i$  is the area of the  $i$ th detector and  $C_i$  is the calibration factor obtained from the single particle pulse height measurement.  $\Delta_i^e$  is the expected density in the  $i$ th detector which is calculated by

substituting the estimated shower parameters in the NKG function and  $W_i$  is the statistical weight factor which is taken as

$$W_i = (1/\sigma_{\text{poisson}}^2)$$

The condition of minimisation of  $\chi^2$  with respect to shower parameters is given by

$$\delta\chi^2 / \delta Q_i = 0$$

where  $i = 1$  to 4 and  $Q_i$ 's are four shower parameters. The above equations are highly non linear and difficult to solve analytically. So independent estimation of the shower parameters are not possible from the above equations. Hence an iterative procedure is applied to estimate the parameters. An iterative process of determining the shower parameters is to adjust the value of shower parameters such that the value of  $\chi^2$  becomes minimum. In the present analysis the quantity  $\chi^2$  is minimised by using the standard method of steepest descent and the values of  $x_0$ ,  $y_0$ ,  $s$  and  $N_e$  for each shower are determined.

#### Study on shower front curvature :

It is well known that the leading particles in the shower front do not lie on a plane and the time spreads of the shower particles in the shower front increases with core distances (4). Due to the nearly cone like shape of the shower front a systematic inclination of the fitted shower direction is expected if the shower front is approximated by a plane and if sampling of the time information are not systematic around the shower core. Shower disk thickness is also a function of the core distance and as a result the spread of the time distribution increases with core distance. In the present experiment an attempt has been made to determine the shower front curvature and the variation of time spreads of the shower particles in the shower front with core distances the following method.

A preliminary arrival direction of the shower is determined by fitting an unweighted plane to the arrival time of shower particles of those detectors which are within 15 m from the shower core provided number of such detectors in the shower event are at least four. The plane approximation of the shower front may be used for small core distances. The deviation of arrival

times from the plane front for the remaining detectors are calculated and the mean measured delays of the shower particles at different core distances are estimated. The mean delays from the plane approximation of the shower front as a function of core distances is shown in fig 2.2.2 . It is found that the mean deviation increases with the increase of core distance, consistent with the results of the Haverah park group (4) and the monte carlo simulation results of Hillas (5) , but the observed variation is not very smooth. This is probably because a small number of timing detectors are used in the present experiment to get the timing information of shower particles. The variation can be expressed by a linear relation of the type

$$dt = a r + c$$

The least squares fit of the results to a straight line gives the value of  $a = 0.19$  and  $c = -2.12$  .

The r.m.s. deviation of arrival times with the core distance is shown in fig 2.2.3 for two different shower sizes. It is observed that the time spread increases with the increase of core distance but decreases with the increase of shower size. The observed spread is compared with the Linsley's formula (6) (a dashed line in the fig 2. ) which is given by

$$\sigma_t = \sigma_0 / n^b (1 + r/r_t)^b$$

with  $\sigma_0 = 2.6$  ns ,  $r_t = 30$  m and  $b = 1.5$  ,  $n$  is the number of particles that hit the detector . In the Fig 2.  $n$  is taken as the particle density corresponding to a shower of  $N_e = 2.5 \times 10^5$  and 'age' 1.3. The observed spread is found slightly greater than that given by the Linsley's formula.

### 3. Re-estimation of the arrival direction :

The shower core position is used to refit the timing informations for all the detectors. Using conical shower front and radial distance dependent weight factors the arrival directions of each shower event are recalculated. The weight factor used in the analysis is given by

$$w_i = 1/\sigma_{total}^2$$

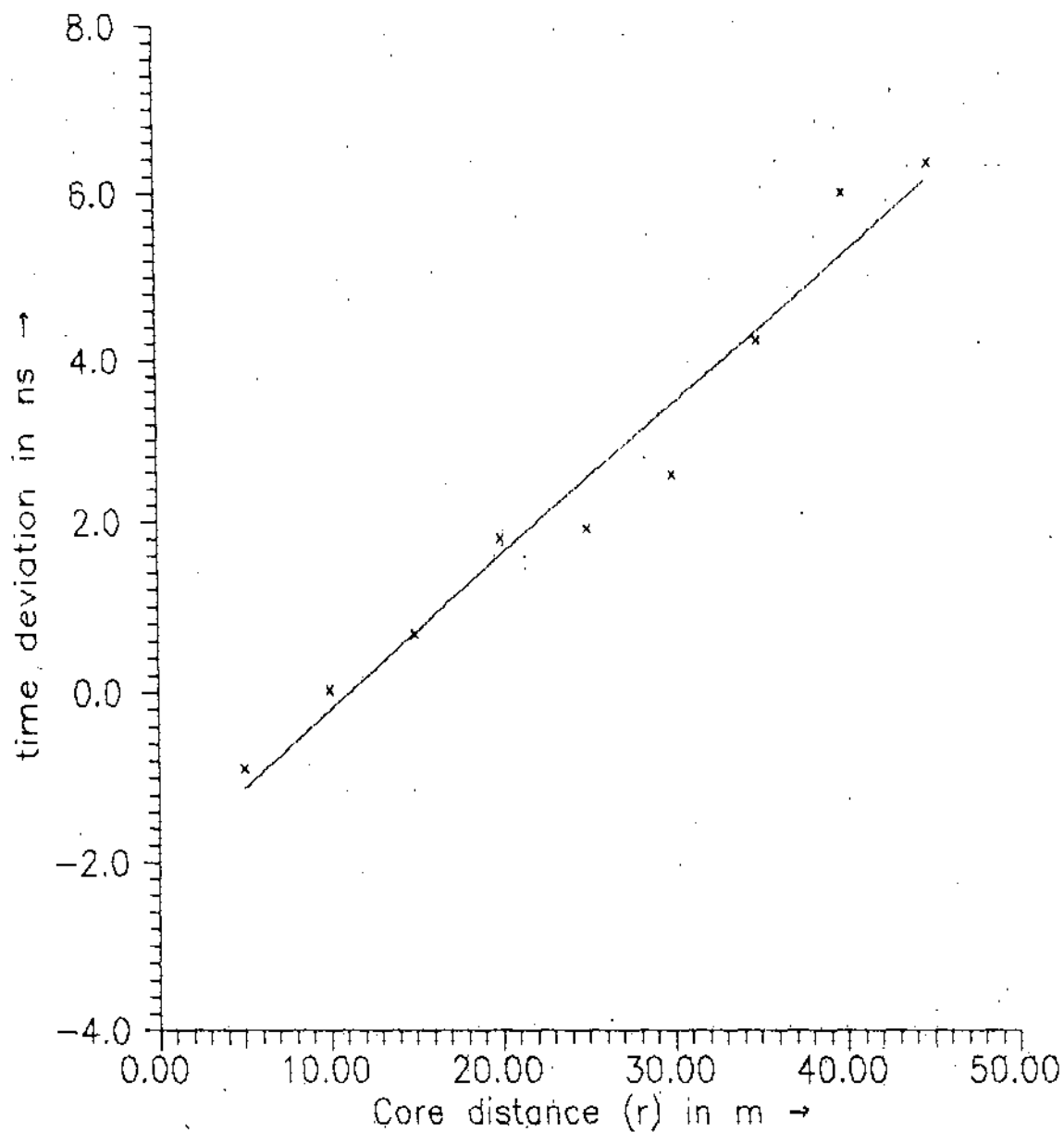


Fig 2.2.2 Variation of mean deviation of arrival times from a plane shower front with core distances. The solid line is the least square fit of the data to a straight line.

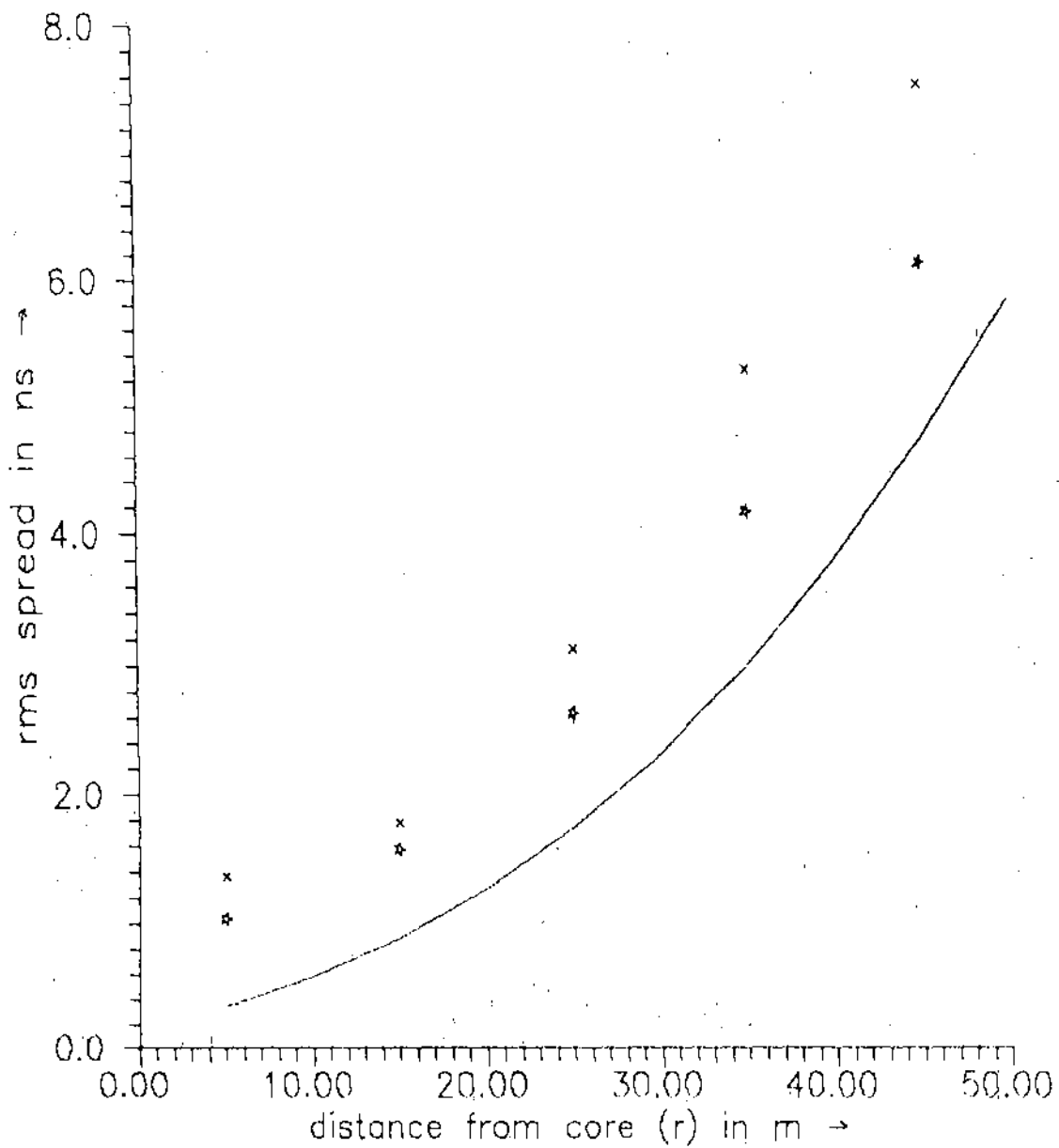


Fig 2.2.3 Variation of rms spread of arrival times with core distances for two shower size range, x -  $N_e < 2 \times 10^5$ , \* -  $N_e > 2 \times 10^5$ . The solid curve represents Linsley's formula (for shower size  $N_e = 2.5 \times 10^5$ , and shower 'age'  $s = 1.3$ ).

where

$$\sigma_{\text{total}}^2 = \sigma_t^2 + \sigma_{\text{inst}}^2 + \sigma_{\text{electronics}}^2$$

An accepted timing fit to a shower front is judged by the value of the quantity

$$\chi_r^2 = 1/(n-3) \sum w_i (t_i^o - t_i^e)^2$$

where  $t_i^o$ ,  $t_i^e$  are the observed and expected time at the  $i$ th detector respectively,  $n$  is the number of timing detectors fired in the shower event and is also judged by the deviation of the measured times,  $dt_i = t_i^o - t_i^e$ , of different detectors. If  $\chi_r^2 > 5$  or any  $dt_i > 3$  then events are reanalyzed after rejecting the most deviant detector. The process is repeated until  $\chi_r^2 < 5$  and all  $dt_i < 3$  or if the events have not remained in four time-measurements of the shower front.

Examples of observed shower data and reconstructed shower parameters from the observed data for two typical observed EAS events are shown in Fig. 2.2.4 and Fig. 2.25.

#### Arrival direction in equatorial co-ordinate system :

During the diurnal motion of a heavenly body its altitude and azimuth continually changes. Also even at the same instant, at places of different latitudes the same body has different altitudes and azimuths. However right ascension and declination of a heavenly body remain the same during their diurnal motion. So 'equatorial co-ordinates' are normally used to define the position of a star.

If the observer's latitude is  $\phi$  and the  $z$  and  $A$  are the zenith and azimuth of a heavenly body then its declination is given by

$$\delta = \text{Sin}^{-1}(\text{Sin}\phi \text{Cos}z + \text{Cos}\phi \text{Sin}z \text{Cos}A) \quad \dots\dots$$

and if  $h$  be its hour angle then

$$h = \text{Sin}^{-1}(\text{Sin}z \text{Sin}A / \text{Cos}\delta) \quad \dots\dots$$

If a heavenly body is observed at local sidereal time  $l$ st and  $h$  is the hour angle of the body then the

Event No 6064

The event time = 3 hr 12.4 minute (Local Siderial time) , Date = 22.03.94

Zenith angle = 18.6° Declination = 19.4°

Azimuthal angle = 250.7° Right Ascension = 209.5°

Chi-square/degrees of freedom = 1.05 (for timing data fit)

Shower Core  $X_0 = 6.0$  m Shower Age (S) = 1.64

$Y_0 = 13.5$  m Shower Size  $N_0 = 2.0 \times 10^5$

Chi-square/degrees of freedom = 0.80 (for density data fit)

Core distance (r) in m	Observed density ln particles/m <sup>2</sup>	Fitted density ln particles/m <sup>2</sup>
11.2	16.0	13.3
6.2	16.0	19.3
28.8	4.0	5.7
15.7	8.0	10.3
10.5	16.0	13.9
5.6	20.0	20.4
15.2	8.0	10.6
8.1	16.0	16.4
18.3	8.0	9.0
20.2	8.0	8.3
34.1	8.0	4.7

\*8(4.7)

\*8(10.9)

\*16(13.9)

\*8(9.0)

\*8(10.9)

\*4(5.7)

++

\*16(19.3)

\*16(16.4)

\*20(20.4)

\*16(13.3)

\*8(8.3)

N  
W \_ | \_ E  
|  
S

Fig 2.2.4a. Observed shower data and reconstructed shower parameters from the observed data

Event No = 1700

Event time = 1 hr 40.4 minute (Local Sidereal time), Date = 27.01.94

Zenith angle = 28.4° Declination = 47.9°

Azimuthal angle = 35.4° Right Ascension = 49.3°

Chi-square/(degrees of freedom) = 1.03 (for timing data fit)

Shower Core  $X_0 = 28.0$  m Shower Age  $s = 1.18$

$Y_0 = 13.0$  m Shower Size  $N_0 = 1.1 \times 10^5$

Chi-square/(degrees of freedom) = 2.12

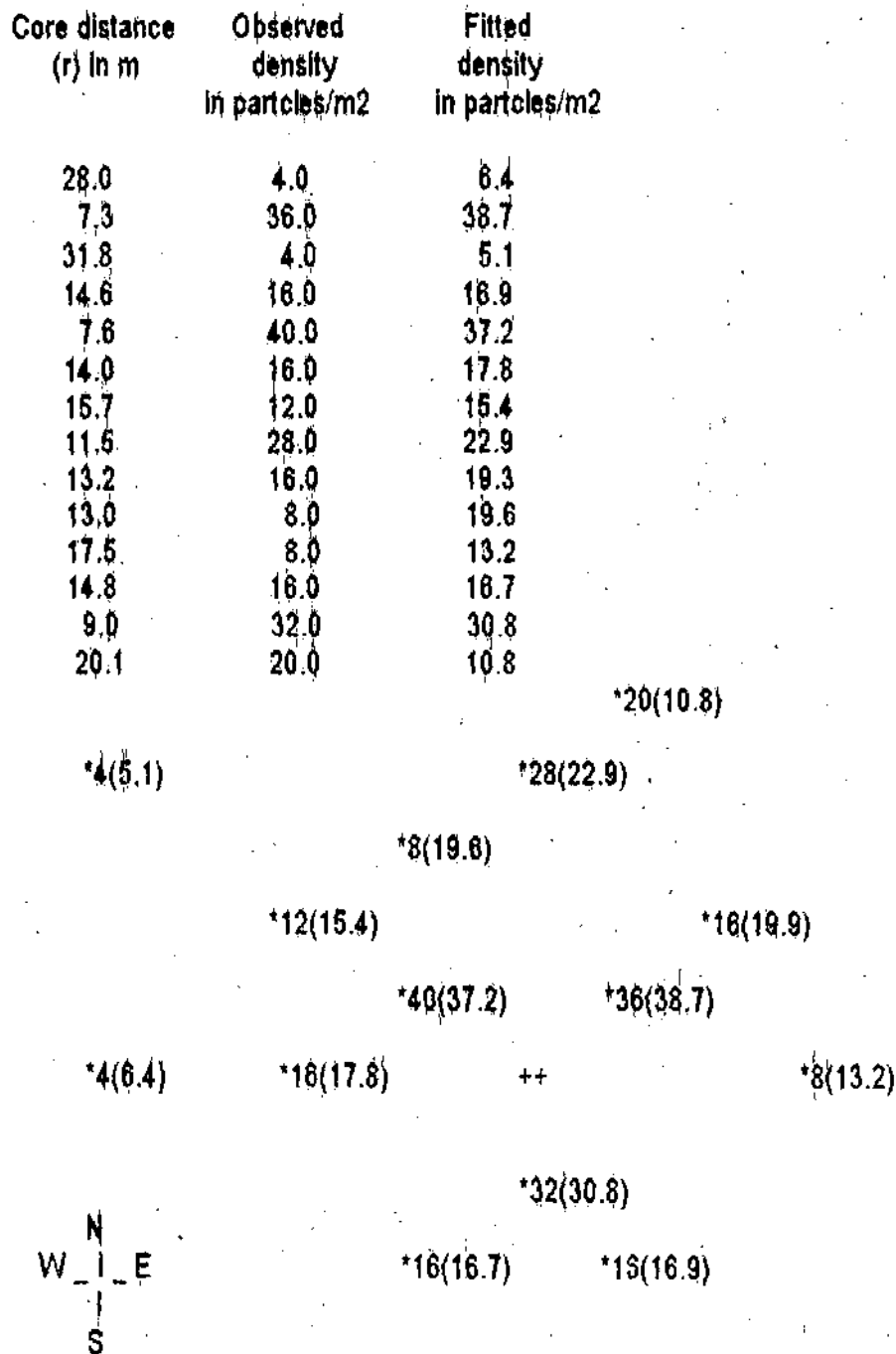


Fig 2.2.4b. Observed shower data and reconstructed shower parameters from the observed data

right ascension of the body  $\alpha$  is given by

$$\alpha = \text{lst} - h$$

### 2.3 Precision of the measurements:

It is evident that any feature of EAS will be affected by the errors in estimation of the shower parameters. In order to estimate the errors in shower parameters as measured by the array and to ascertain any systematic biases in the analysis of air shower events artificial air shower events are simulated and then the simulated data are analysed with usual analysis programme. By selecting random shower sizes from an incident power law shower size spectrum ( $N^{-2.5}$ ) with zenith angle modulated of  $\text{Cos}^7z$  in the size range  $10^4 - 10^7$  showers have been simulated and randomly projected over an area (a circular area of radius 40m with centre in coincidence with the array centre) approximately twice that of the array. The charged particles of EAS are expected to follow NKG distribution function. Poission fluctuation on recorded particle numbers have been incorporated. These simulated events are then analysed and interpreted using the same methods and criteria that are employed with genuine data. From the simulation study it is found that there is no systematic biases in the analysis procedure employed in the experiment. The distribution of differences between the simulated parameters and fitted parameters are shown in fig.2.3.1. The width of these distributions give the error in the estimation of the corresponding shower parameters which are as follows

- i) Uncertainty in Core location (a)  $\delta x_0 = 2.04 \pm .05$   
 (b)  $\delta y_0 = 2.16 \pm .05$   
 ii) Uncertainty in shower size  $\delta N_0/N_0 = (15.6 \pm .3) \%$

and iii) the value age parameter is uncertain by  $\delta s = .109 \pm .002$

The  $\chi^2$  distribution for the experimentally observed that and that obtained from the analysis of the artificial shower data are shown in fig.2.3.2.

#### Angular Resolution of the NBU EAS array :

An exact determination of arrival direction of shower is especially important to identify point sources. Some error is introduced in the estimated arrival direction due to instrumental uncertainty of the time measuring instruments, time spread of shower particles in shower disk, finite number of time measuring detectors etc. The accuracy in the measurement of angular co-ordinates

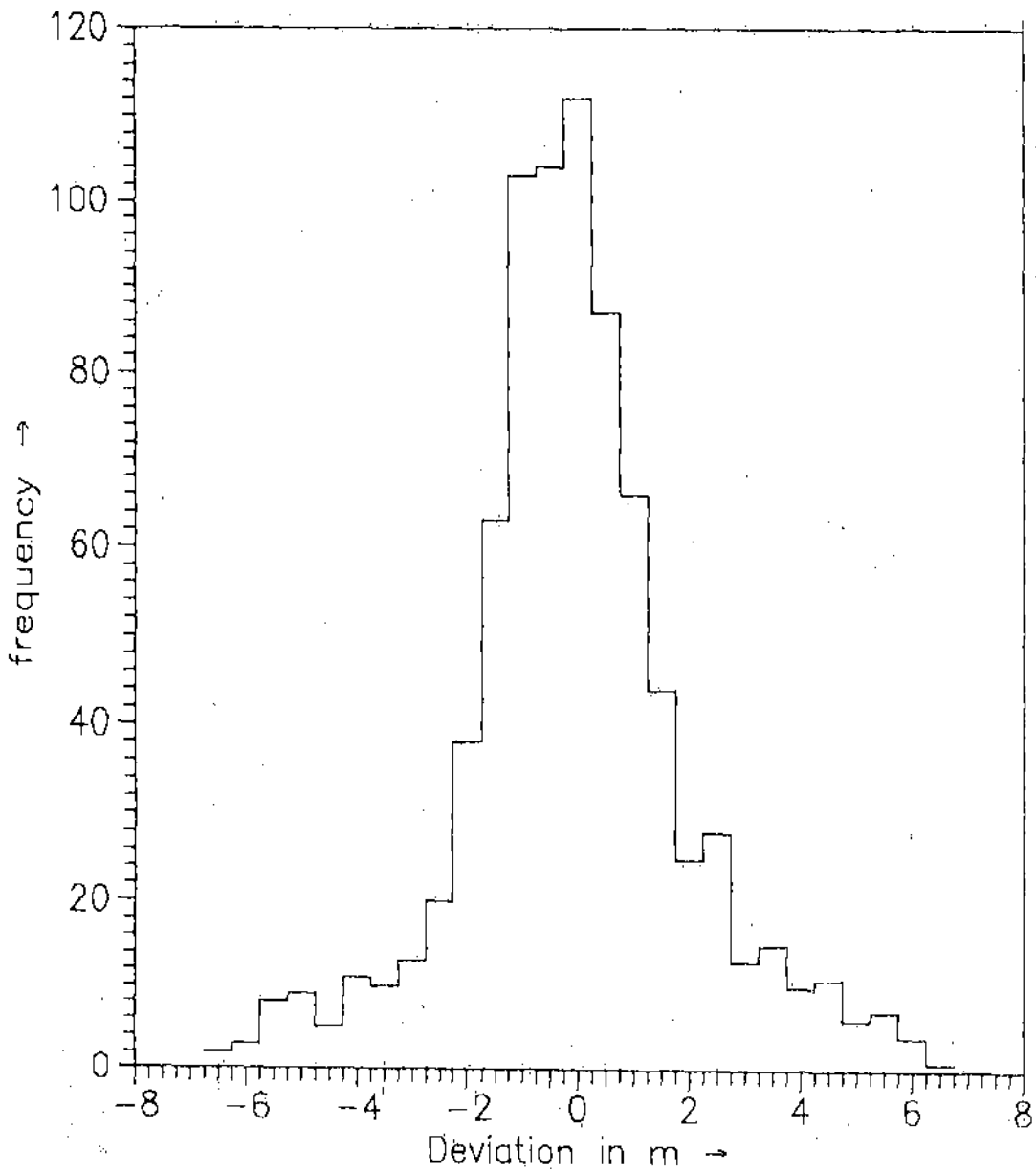


Fig 2.3.1a Distribution of deviations of the estimated core (x) from the true core position (from simulation results).

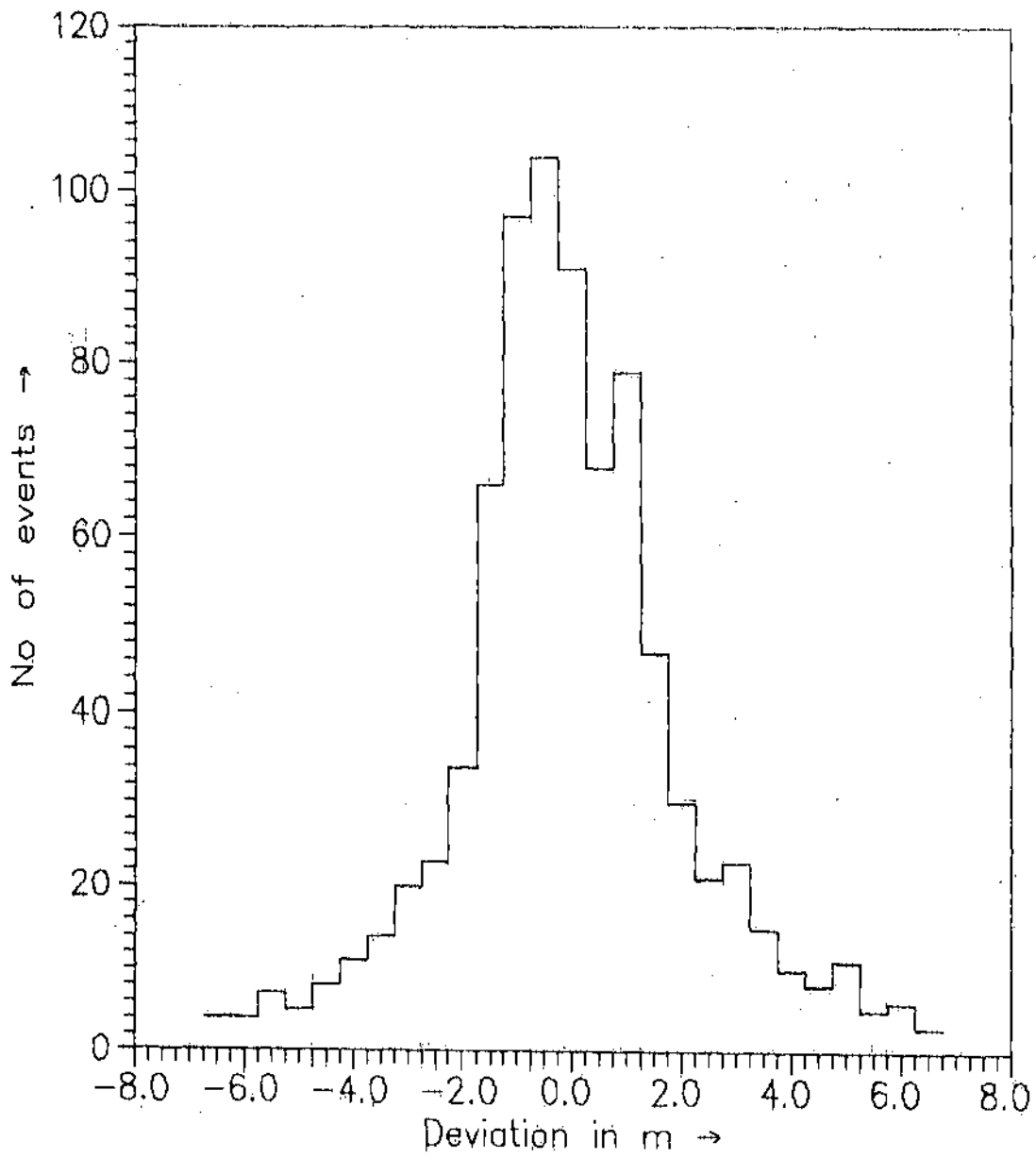


Fig 2.3.1b Distribution of deviations of the estimated core (y) from the true core position (from simulation results).

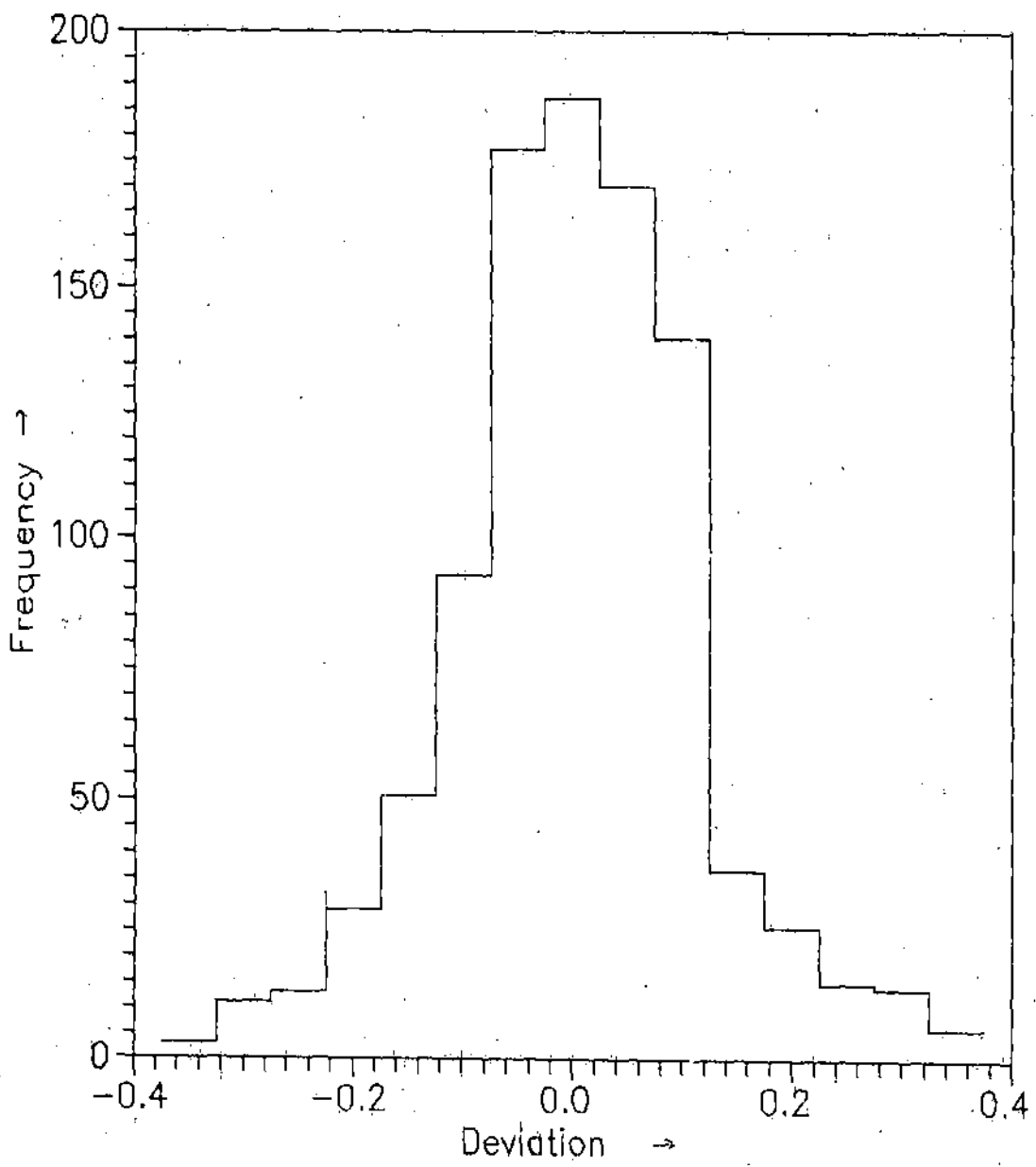


Fig 2.3.1c Distribution of deviations of the estimated age (s) from the true age (from the simulation results).

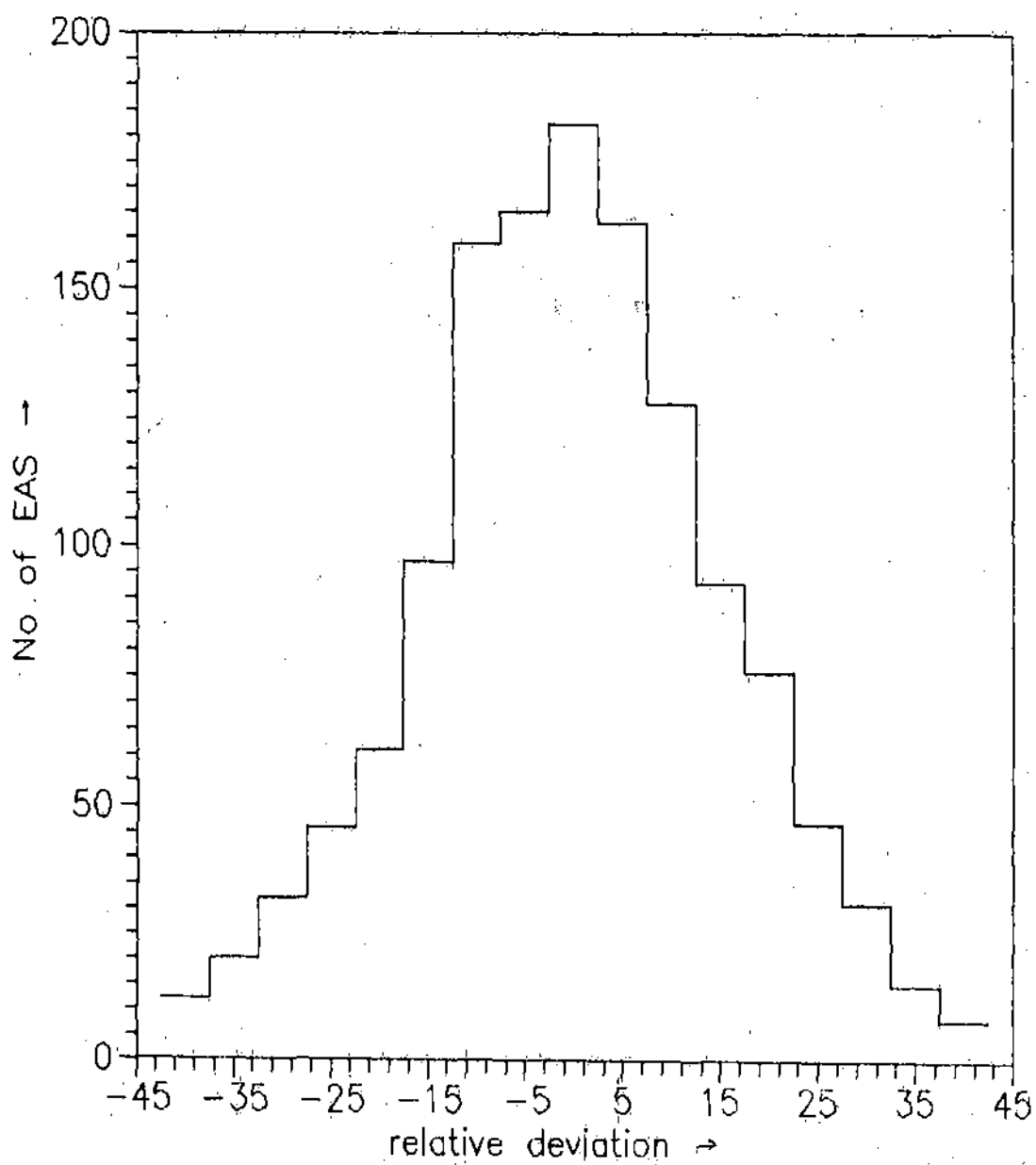


Fig 2.3.1d Distribution of relative deviations of the estimated size ( $N_{\hat{a}}$ ) from the true shower size (from simulation results).

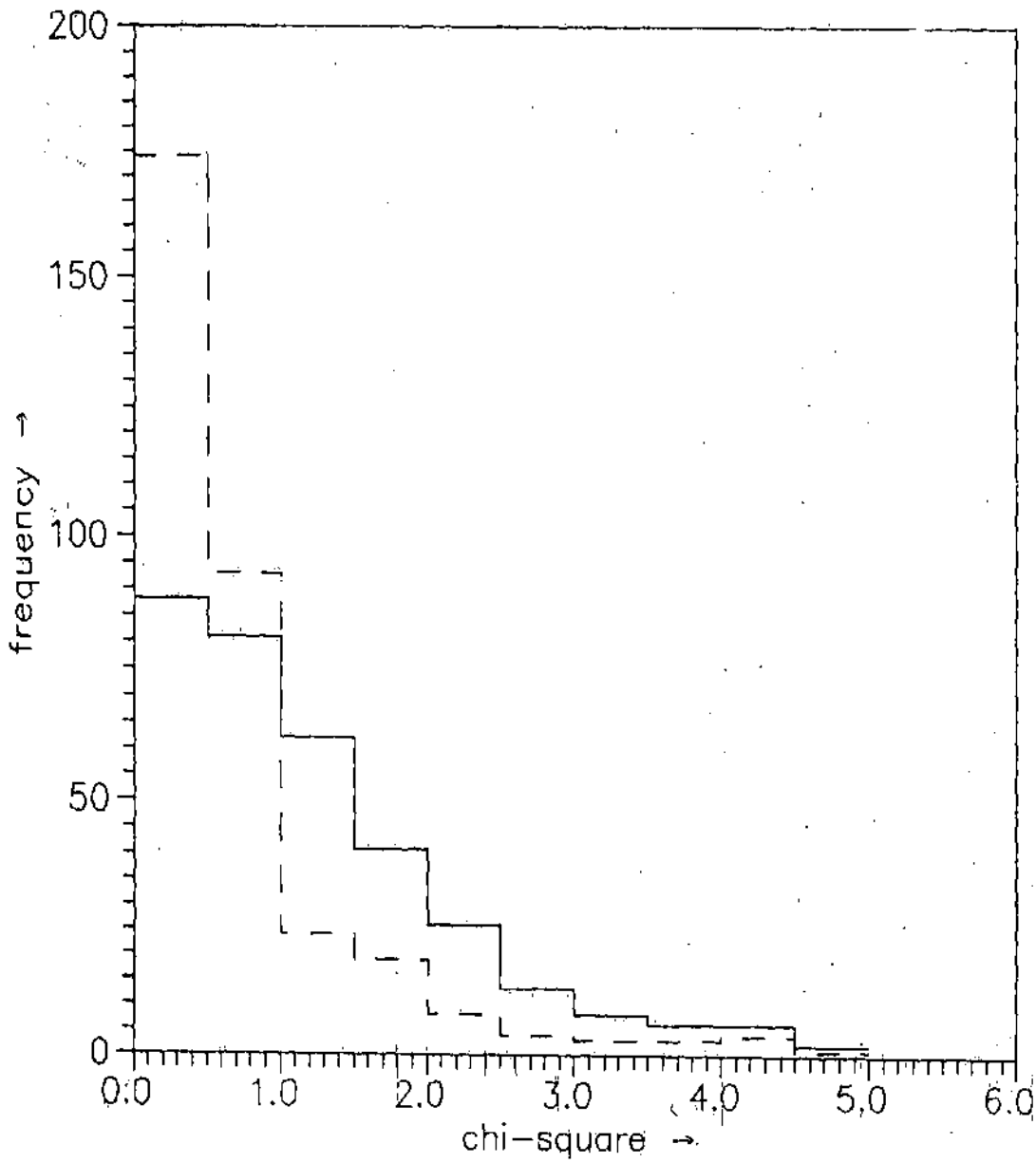


Fig 2.3.2 Chi-square distributions for experimentally observed shower data (solid line) and for artificial shower data (dashed line).

i.e, angular resolution of an air shower array is thus a very important parameter to estimate. In the absence of a point like source in UHE range which can serve as a steady candle the angular resolution of the NBU EAS array has been estimated by the conventional 'split array' method. For the determination of angular resolution only those shower events are selected in which all the eight fast timing detectors give information about the relative times of shower front particles. The total eight detectors are divided into two sets (even and odd detectors) and two independent estimate of the arrival direction of the same event has been made from two sub-arrays. The mean space angle difference ( $d\psi$ ) between the two arrival direction is calculated. The frequency distribution of differences ( $d\psi$ ) is shown in fig 2.3.4. The frequency distributions of differences in zenith angle, azimuthal angle and in equatorial co-ordinates are shown in fig.2.3.5. The width of the Gaussian fitting of these distributions give the uncertainty in measurements of corresponding parameters. Since error in determining angular co-ordinates from the two independent sub-arrays added quadratically in the resulting distribution and there are twice as many detectors in the whole array then the individual sub-arrays so the angular resolution of the whole array will be  $1/2^{1.5}$  times of the width of the distribution. The resolution of the array in different angular co-ordinates is shown in table 1.

Table 1

Angular Co-ordinates	Zenith	Azimuth	Declination	Right-ascension
Resolution from Experimental data	$1.10^{\circ} \pm .02^{\circ}$	$1.99^{\circ} \pm .03^{\circ}$	$1.10^{\circ} \pm .02^{\circ}$	$1.44^{\circ} \pm .03^{\circ}$
Resolution from Simulation data	$0.55^{\circ} \pm .02^{\circ}$	$1.65^{\circ} \pm .07^{\circ}$	$0.54^{\circ} \pm .02^{\circ}$	$1.03^{\circ} \pm .04^{\circ}$

It is found that the resolution of the array is not very good in azimuth. This is probably due to small number of detectors used for the time measurement. In order to check the resolution of the array Monte Carlo simulation have been carried out. Particle arrival times were generated using the

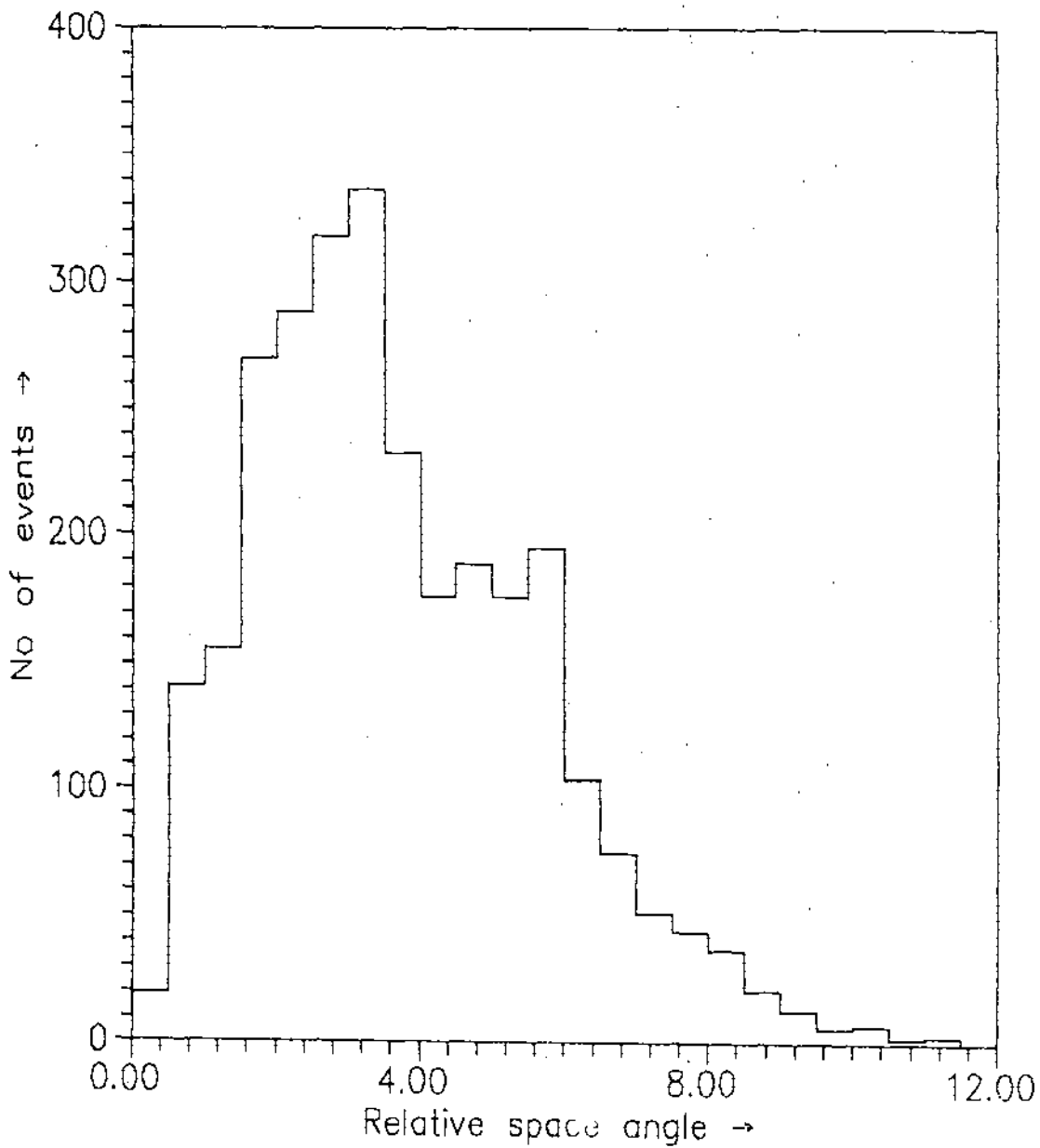


Fig 2.3.4a Distribution of relative space angle measured by two sub arrays for weighted curved shower front.

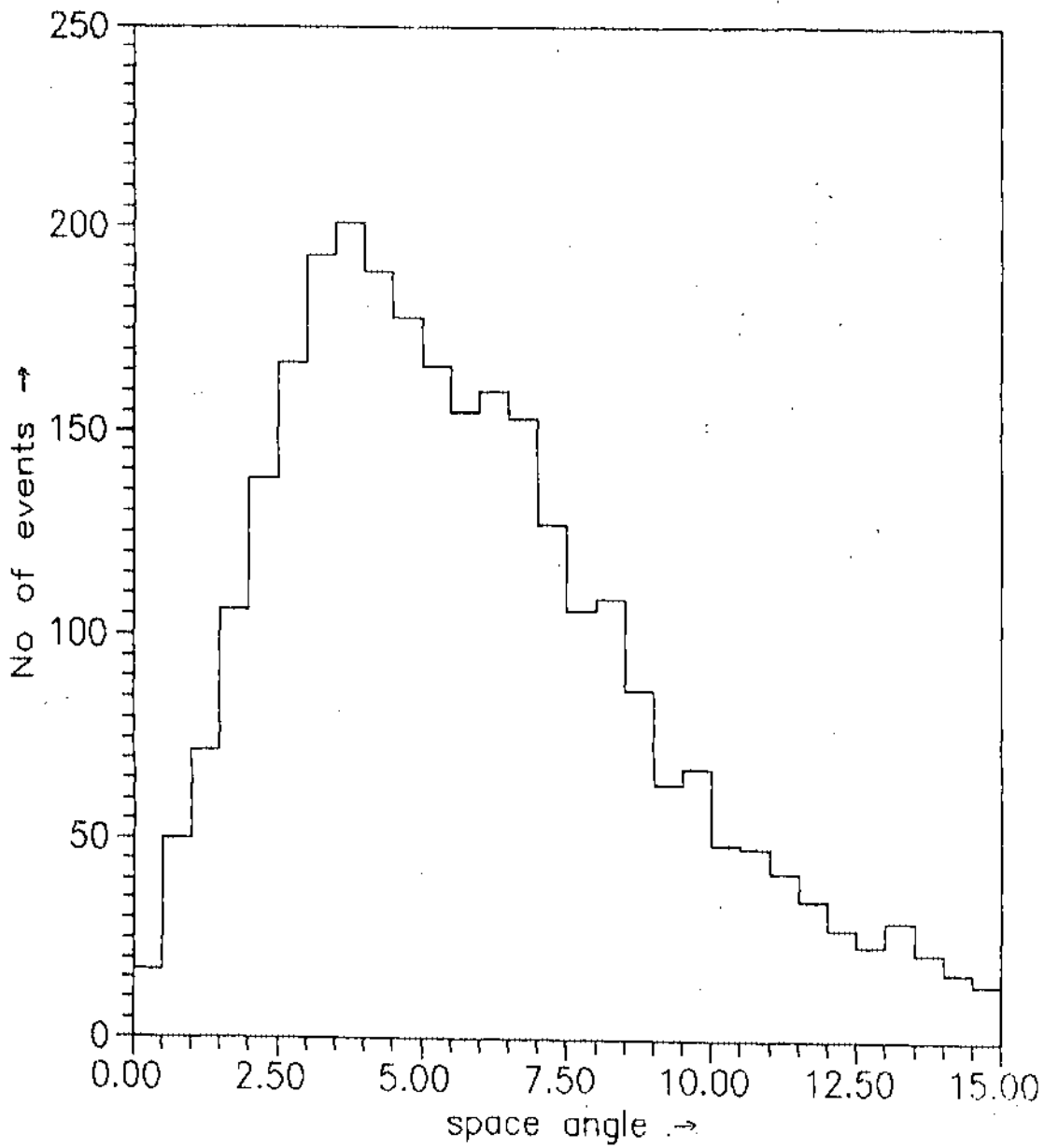


Fig 2.3.4b Distribution of relative space angles measured by two sub arrays for an unweighted plane shower front fit of arrival times.

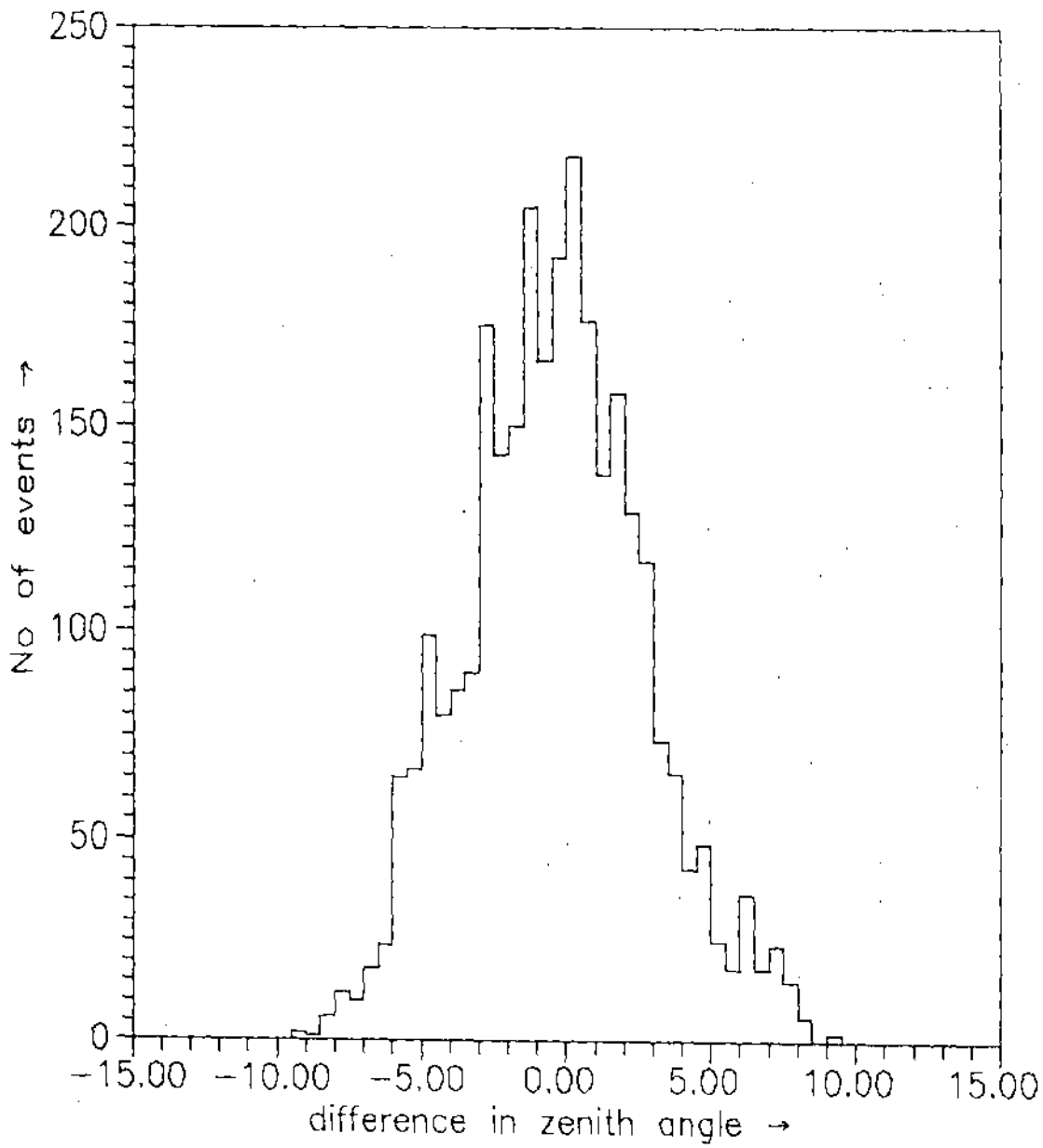


Fig 2.3.5a Distribution of relative deviations in Zenith angle.  
(Average =  $-0.37 \pm 0.06$ , sigma =  $3.12 \pm 0.04$ )

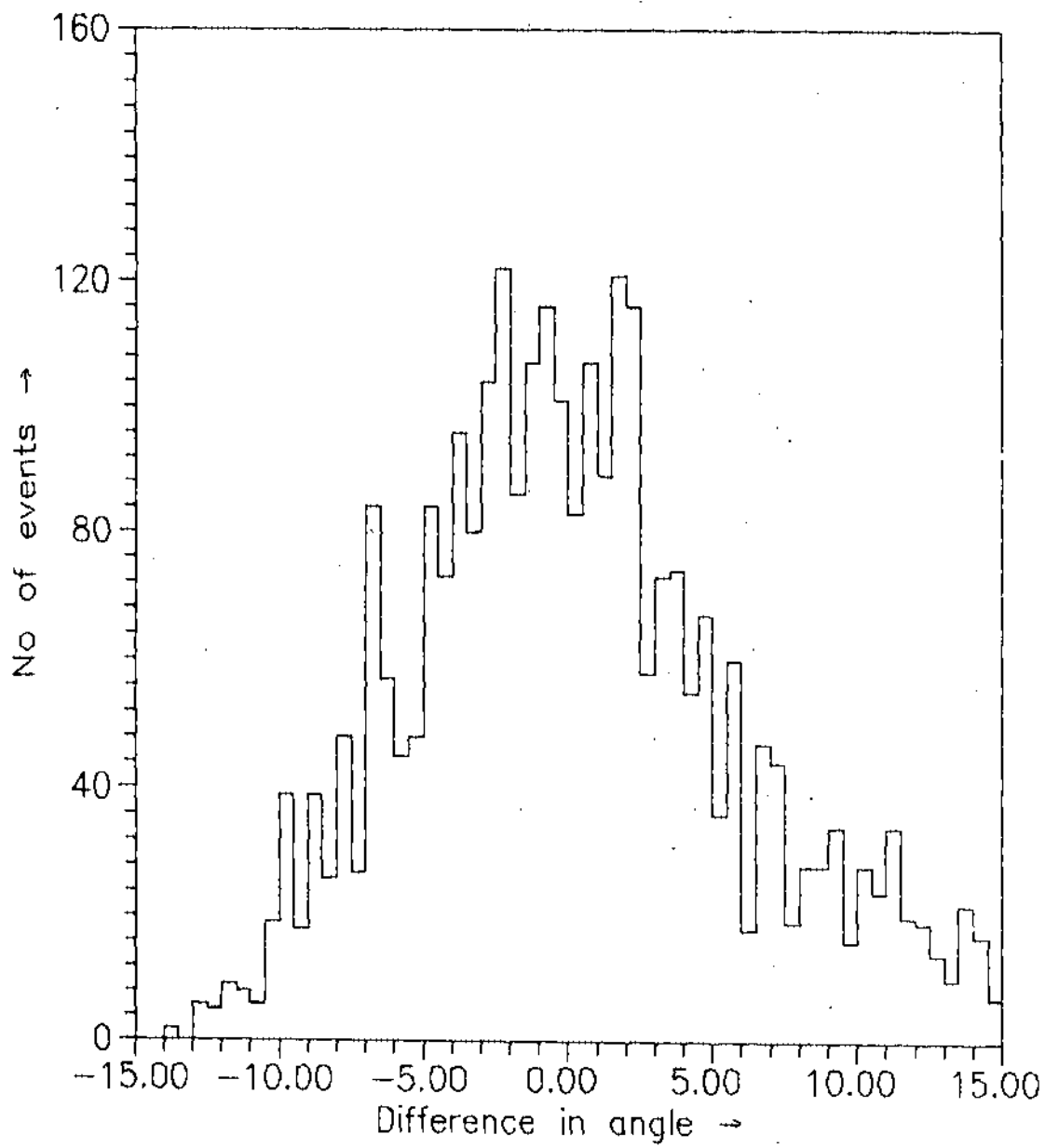


Fig 2.3.5b Distribution of relative deviations  
 in Azimuth angle  
 Average =  $0.2 \pm 0.1$  , St.Dev. =  $5.64 \pm .08$

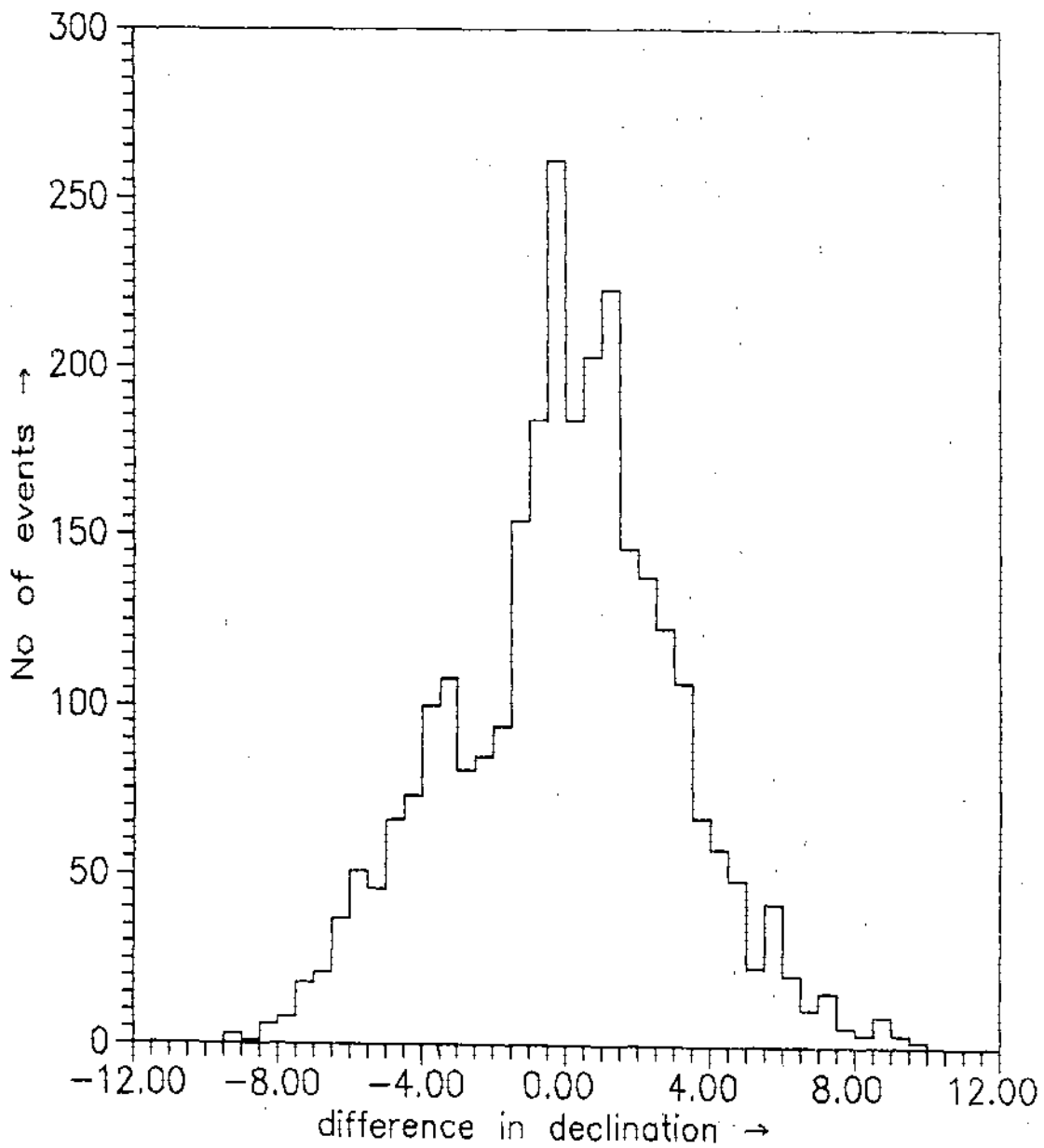


Fig 2.3.5c Distribution of relative deviations in Declination  
(Average =  $-0.05 \pm .06$  , St. Dev. =  $3.11 \pm .04$  )

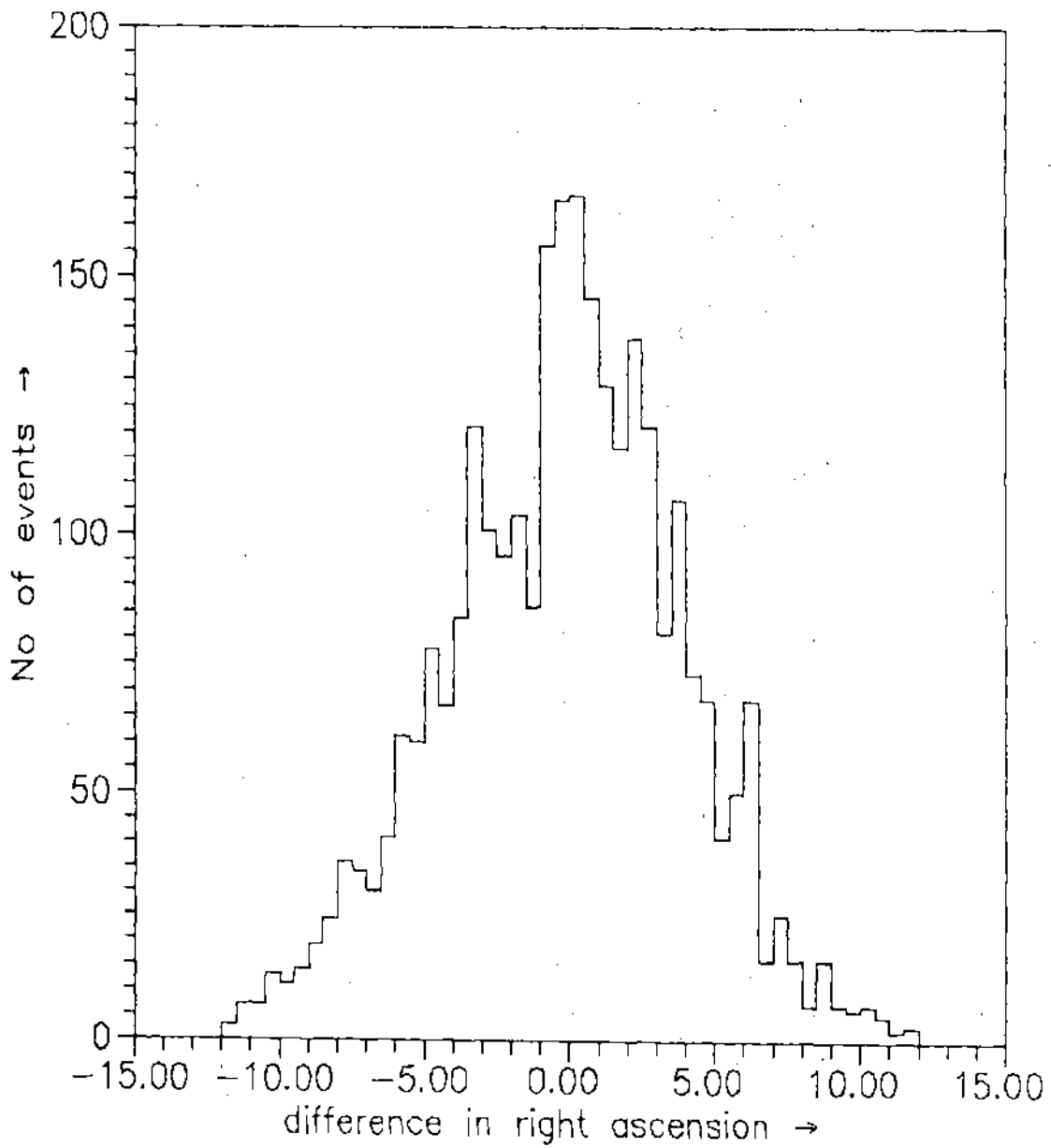


Fig 2.3.5d Distribution of relative deviations in Right Ascension.  
(Average =  $-0.20 \pm 0.08$  , St.Dev. =  $4.08 \pm 0.05$  )

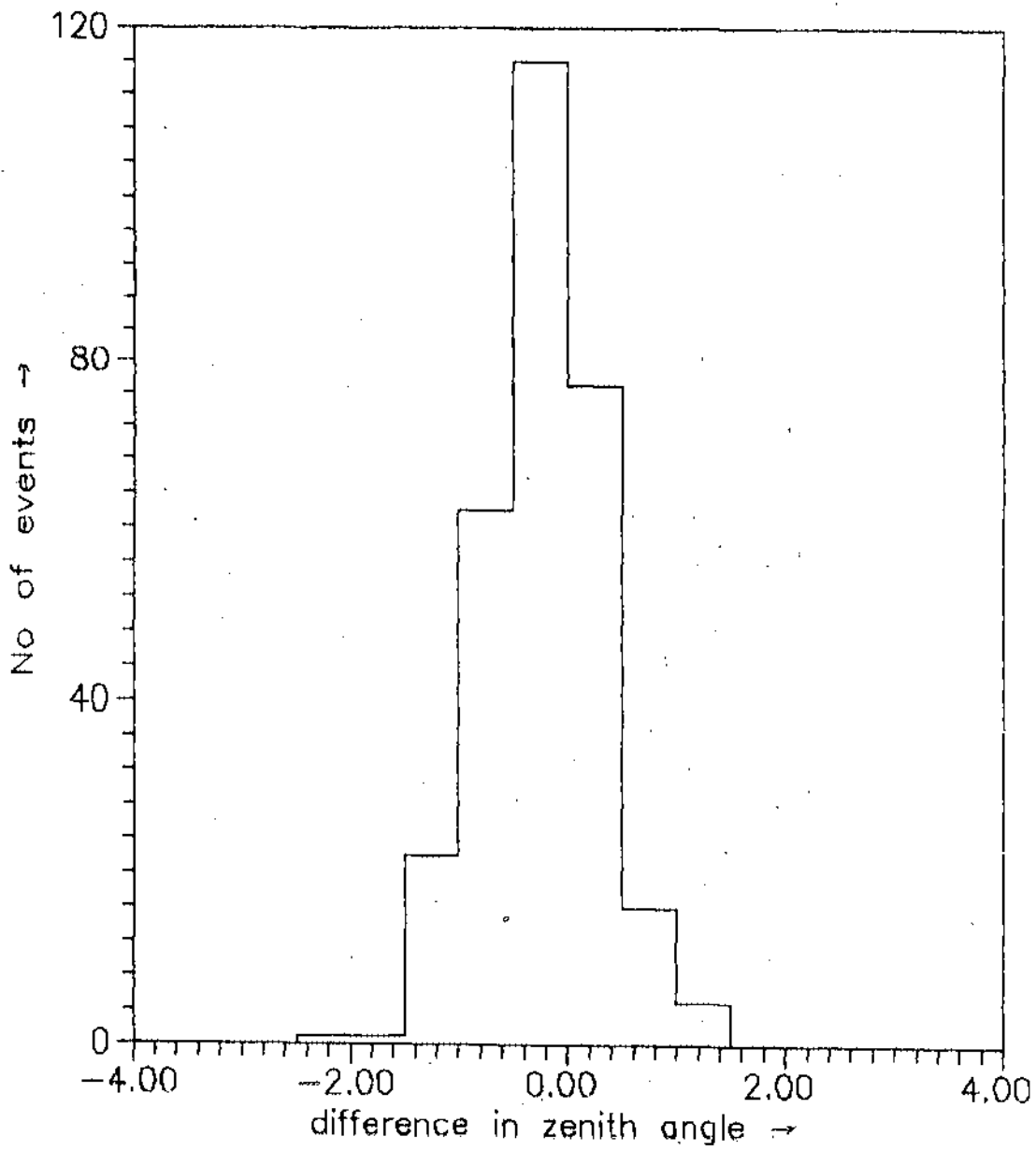


Fig 2.3.6a Distribution of relative deviations in Zenith angle (for simulated data)

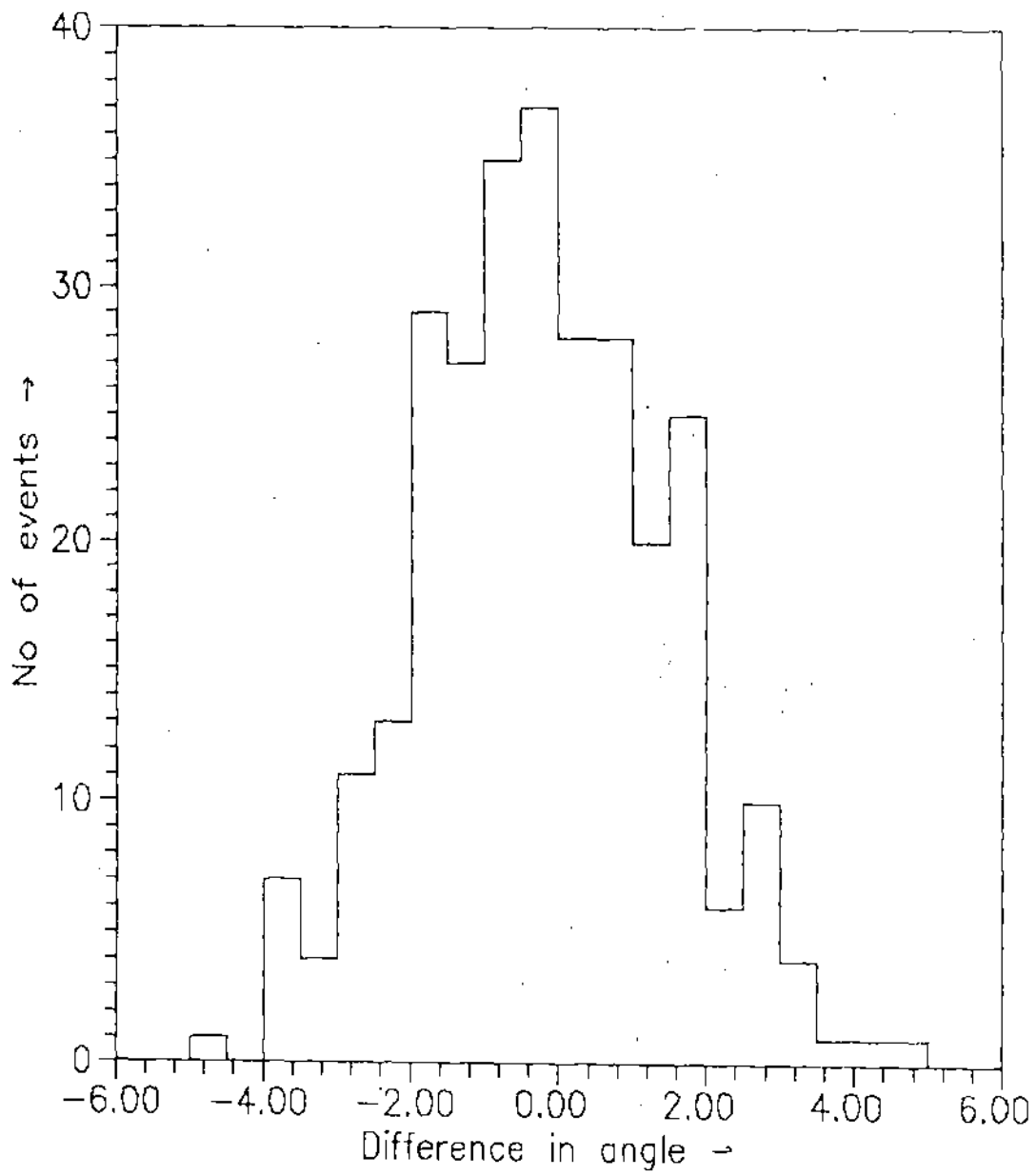


Fig 2.3.6b Distribution of relative deviations in Azimuth angle (for simulated data )

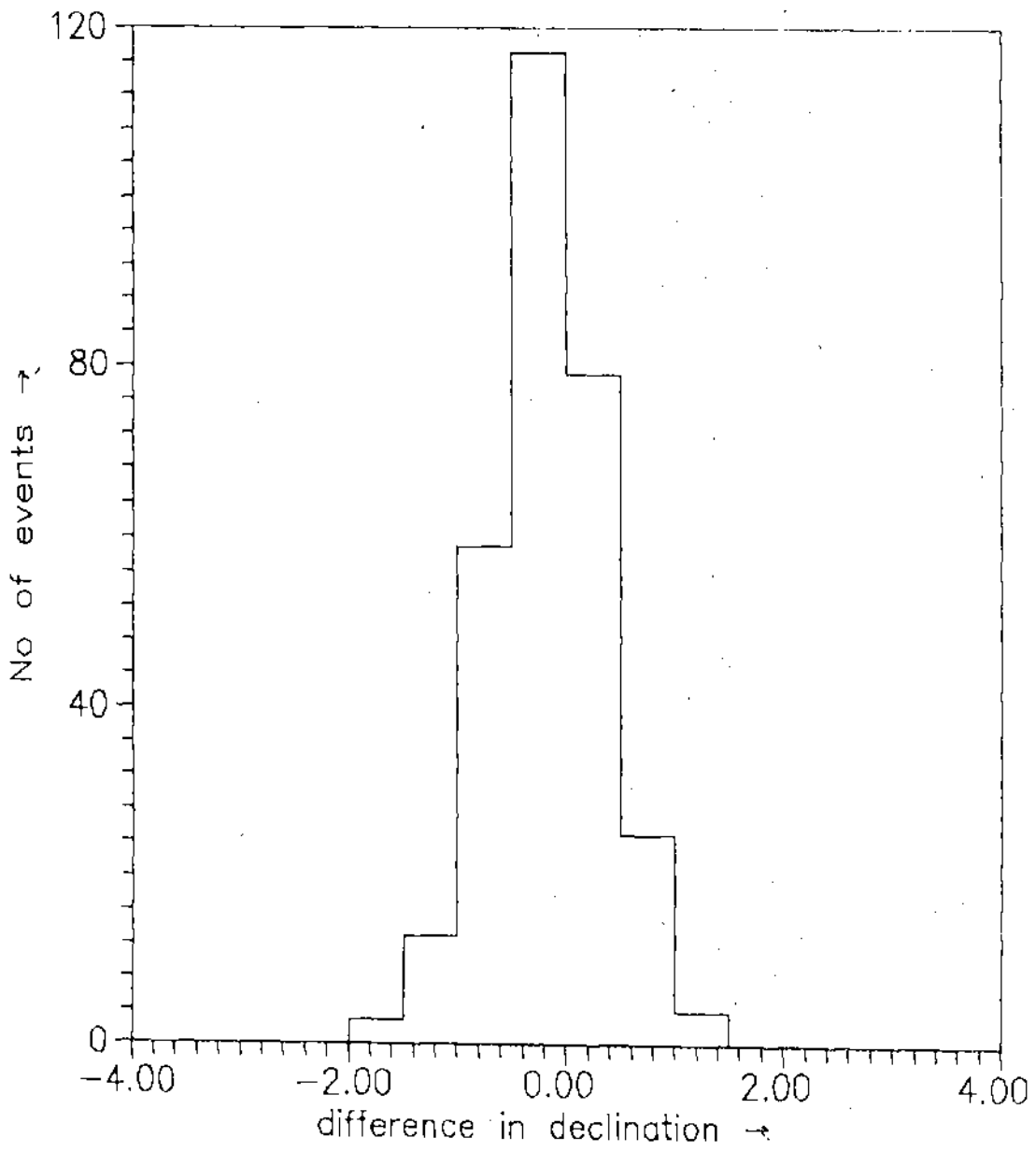


Fig 2.3.6c Distribution of relative deviations in Declination (for simulated data )

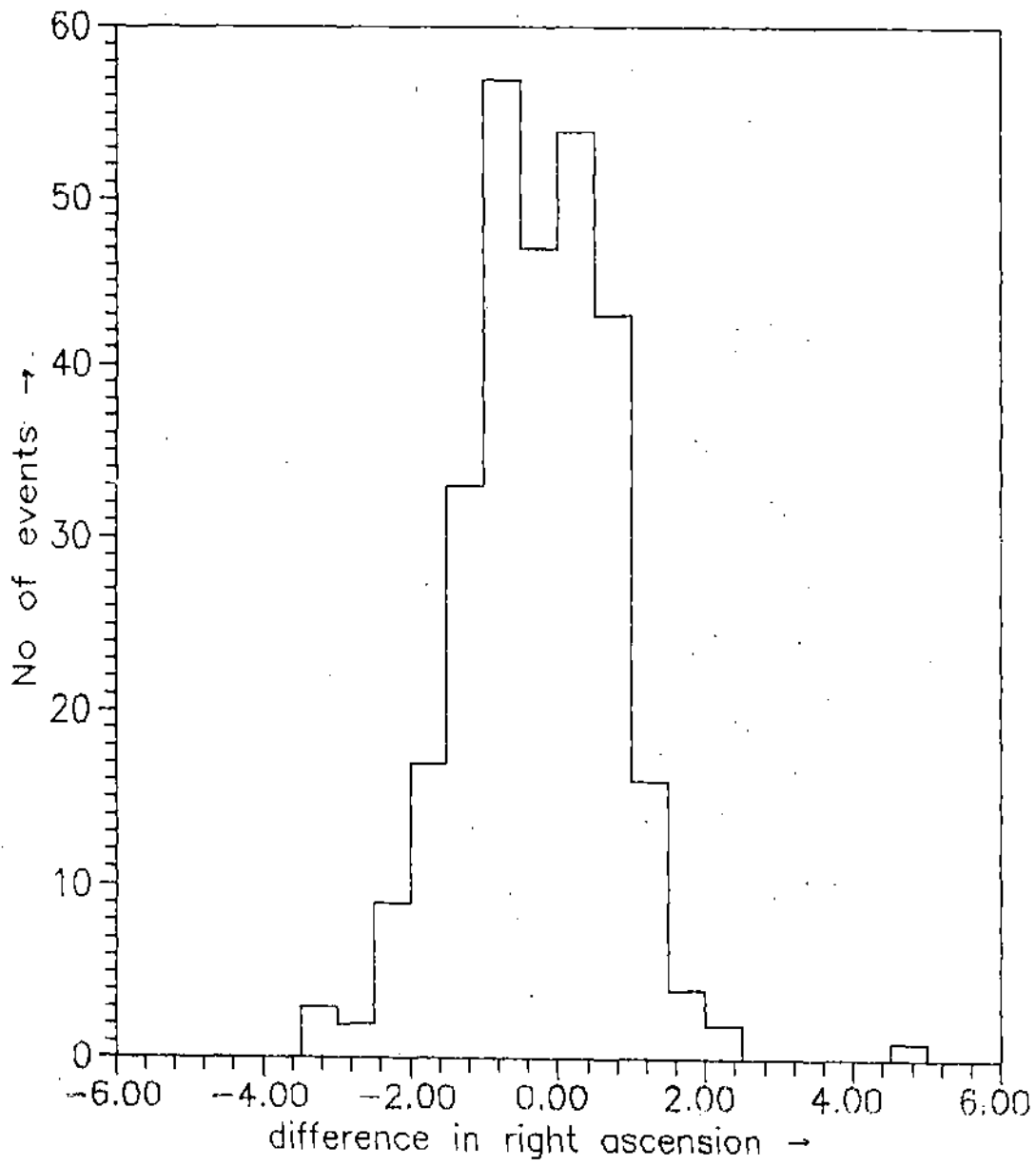


Fig 2.3.6d Distribution of relative deviations in Right Ascension (for simulated data).

observed curvature and the rms spread assuming a Gaussian distribution. The instrumental uncertainty is also included. The event times are selected randomly from the observed event times. The arrival times are then fitted to conical shower front with proper weightage and thus the resolution of the array is estimated. The resolution of the array obtained from the simulation results is also shown in Table 1. It is found that the resolution of the array estimated by the sub-array method is greater than that obtained from simulation results.

The sub-array comparison technique has been employed to compare the following shower front approximation

- 1) An unweighted plane shower front
- 2) A weighted curved shower front

The results are shown in Table 2 and fig.2.3.4 . From the results it is clear that the angular resolution of the array has been improved by a lot by introducing the weights and the curvature.

Table 2

Fit	Mean Space angle	Width
Plane(Unweighted)	$5.78^{\circ} \pm .06^{\circ}$	$3.13^{\circ} \pm .04^{\circ}$
Curve(Weighted)	$3.71^{\circ} \pm .04^{\circ}$	$1.97^{\circ} \pm .03^{\circ}$

#### Projected angle Distribution :

Whether the array co-ordinate system is coincident with the local horizon is checked by using the distribution of arrival angle projected on two orthogonal vertical planes. As the azimuth angle distribution of the showers is uniform, the projected angle distribution is expected to be symmetric about zero value. The observed projected angle distributions are shown in fig 2.3.6 .It is found that the distributions are symmetric about zero, having a mean close to zero and r.m.s. spread of 21.3 and 21.4 in the North-South and East-West planes respectively , consistent with the zenith angle distribution of showers.

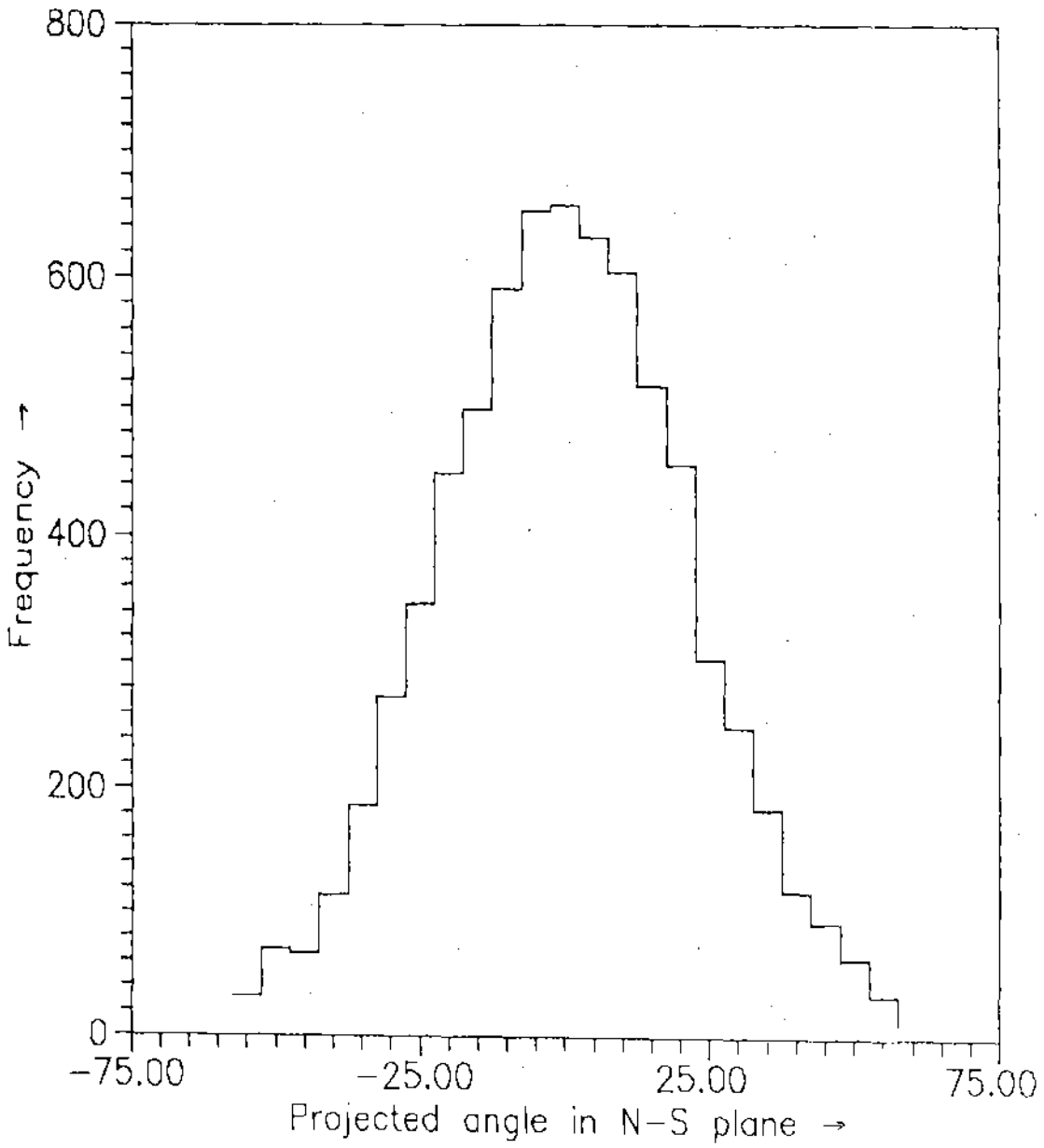


Fig 2.3.7a Projected angle distribution  
in N-S plane.  
(Average =  $-0.03 \pm .25$ )

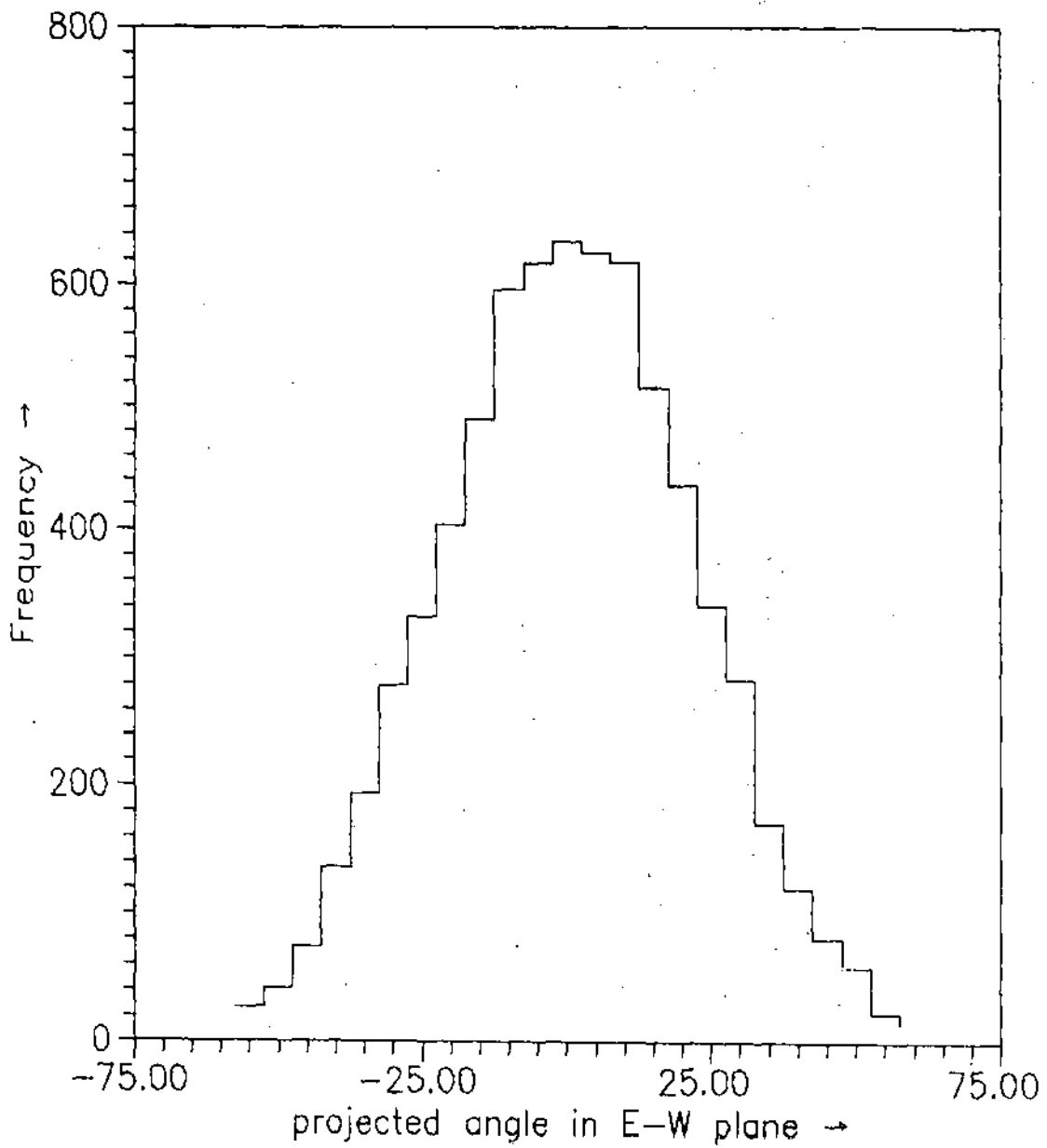


Fig 2.3.7b Projected angle distribution  
in E-W plane.  
( Average =  $0.16 \pm .25$  )

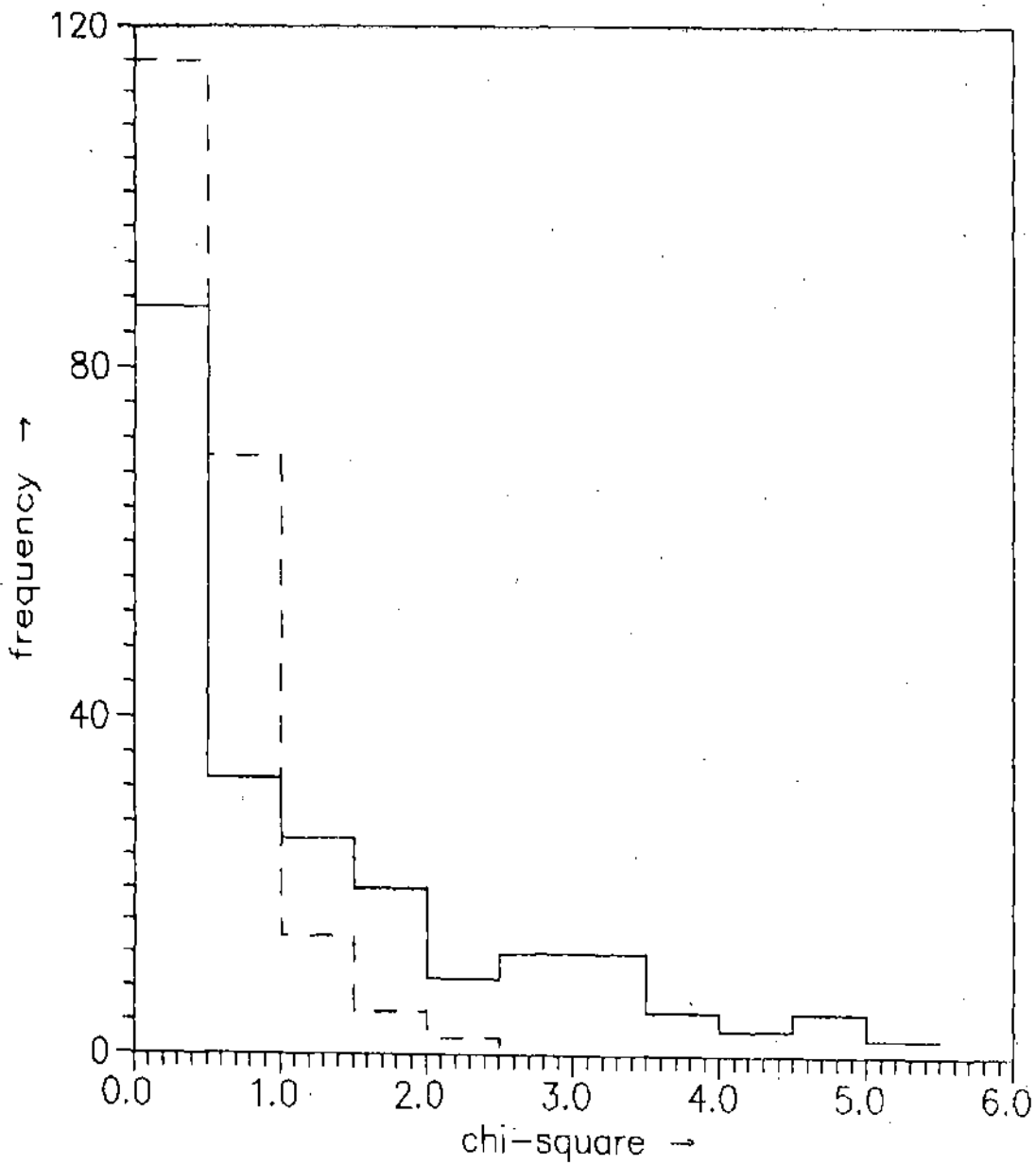


Fig 2.3.8 Chi-square distributions for timing data fit .Solid line - for experimentally observed shower data ,dashed line - for simulated shower data.